https://jssr.ui.ac.ir/?lang=en
Journal of Stratigraphy and Sedimentology Researches
E-ISSN: 2423-8007
Vol. 42, Issue 4, No. 105, 2026, 33-50
Received: 09.09.2026 Accepted: 04.10.2026

Research Paper

Regional synthesis of rare microfacies in the Oligo–Miocene Qom Formation (Iran): Temporal and spatial distribution, depositional environments, and paleogeographic significance

Ebrahim Mohammadi*
Department of Ecology, Institute of Science, High Technology and Environmental Science, Graduate University of Advanced Technology, Kerman, Iran
e.mohammadi@kgut.ac.ir

Mehdi Ghaedi
Nanjing Institute of Geology and Palaeontology, Chinese Academy of Sciences, Nanjing, Jiangsu Province, China
mehdi@nigpas.ac.cn

Abstract
This study investigates the temporal and spatial distribution of rare microfacies of the Qom Formation and their depositional environments. Detailed examination of 15 stratigraphic sections by the first author, together with a comprehensive review of previous studies, demonstrates that, in addition to common microfacies, the Qom Formation contains several rare microfacies with limited spatial distributions. These include turbiditic microfacies, breccia, sandy planktonic foraminiferal wackestone, bioturbated bioclastic wackestone, nummulitid packstone, perforate foraminifera–bryozoan–echinid packstone, coral-bearing, intraclast-bearing, *Neorotalia*-bearing, crinoid grainstone, ooid-bearing, *Gastrochaenolites*-bearing, peloid-bearing, ostracod-bearing, fenestral mudstone, and stromatolitic bindstone microfacies. Some microfacies, such as ooid-rich, fenestral mudstone, and peloid-rich types, are widespread in the Oligocene–Miocene Asmari Formation but occur only sporadically in the Qom Formation. These rare microfacies represent tidal-flat, lagoonal, shoal/barrier, carbonate-slope, normal-marine, and turbiditic-marine settings. Restricted petrofacies also include mixed carbonate–siliciclastic, gravelly, sandy, conglomeratic, evaporitic, and volcanic-bearing types. Most rare microfacies are Early Miocene in age and occur along the margins of the Central Iranian Desert, particularly the Semnan–Garmsar–Qom region, and in northwestern Iran, especially Mianeh–Bostanabad. Their localized distribution indicates that the Qom Sea was not permanently connected to the open marine realm and that progressive restriction and eventual closure of this connection began during the Early Miocene.
Keywords: Qom Formation; Rare microfacies; Oligo–Miocene; Carbonate platform; Tethyan seaway; Petrofacies.

*Corresponding author
Mohammadi E. and Ghaedi M. (2026). Regional synthesis of rare microfacies in the Oligo–Miocene Qom Formation (Iran): Temporal and spatial distribution, depositional environments, and paleogeographic significance. Journal of Stratigraphy and Sedimentology Researches, 42(4): 33-50. https://doi.org/10.22108/jssr.2026.150537.1340

2423-8007 / © 2026 University of Isfahan
This is an open access article under the CC BY-NC-ND 4.0 License (https://creativecommons.org/licenses/by-nc-nd/4.0/).

https://doi.org/10.22108/jssr.2026.150537.1340

Introduction

In this study, microfacies documented from the Qom Formation in only one or two stratigraphic sections, or reported in only one or two published studies, are considered "rare microfacies". A given stratigraphic section may, however, have been investigated and reported in more than one publication; therefore, the number of publications does not necessarily correspond to the number of independent occurrences. This classification is based solely on the limited representation of these microfacies in the published stratigraphic and sedimentological record available to date, irrespective of the underlying reasons for their apparently rare documentation. Accordingly, the term “rare” refers to the frequency with which a microfacies has been documented in the available literature and does not necessarily imply low abundance within the depositional system itself.

Analysis of the spatial and temporal distribution of carbonate microfacies provides fundamental insights into the evolution of depositional systems, platform architecture, and paleoenvironmental conditions. Variations in microfacies assemblages commonly reflect changes in depositional energy, water depth, ecological conditions, accommodation space, and basin configuration, thereby serving as one of the most reliable tools for reconstructing ancient carbonate environments (Hallock et al. 1986; Flügel 2010; Brandano et al. 2022).

The Oligo–Miocene Qom Formation represents one of the most fossiliferous marine successions in Iran and constitutes the principal hydrocarbon-bearing carbonate unit of Central Iran (Mohammadi et al. 2013; Mohammadi 2024a). Owing to its wide geographic distribution and complex tectono-sedimentary history, the formation exhibits pronounced lateral and vertical variations in lithology, thickness, and stratigraphic boundaries across different parts of the basin. Previous studies indicate that deposition of the Qom Formation occurred within three distinct tectono-sedimentary domains, namely the Sanandaj–Sirjan fore-arc basin, the Urumieh–Dokhtar intra-arc basin, and the Central Iran back-arc basin (Mohammadi et al. 2013, 2015, 2019). These tectonic settings exerted a primary control on facies architecture and carbonate platform development.

Rapid lateral facies changes are among the most distinctive characteristics of the Qom Formation. Consequently, several lithostratigraphic members cannot be traced continuously throughout the basin, reflecting strong spatial heterogeneity in depositional environments and sedimentary processes. Although numerous investigations have documented the common microfacies of the Qom Formation, considerably less attention has been paid to rare microfacies characterized by restricted geographic and stratigraphic occurrence. Nevertheless, these uncommon microfacies may provide critical evidence for localized depositional conditions, short-lived environmental events, or particular stages in platform evolution that cannot be inferred from the dominant facies alone.

Based on detailed microfacies analysis of 15 stratigraphic sections by the first author (and co-authors), together with a comprehensive review of previously published studies, several rare microfacies are recognized as occurring sporadically throughout the Qom Formation.

https://doi.org/10.22108/jssr.2026.150537.1340

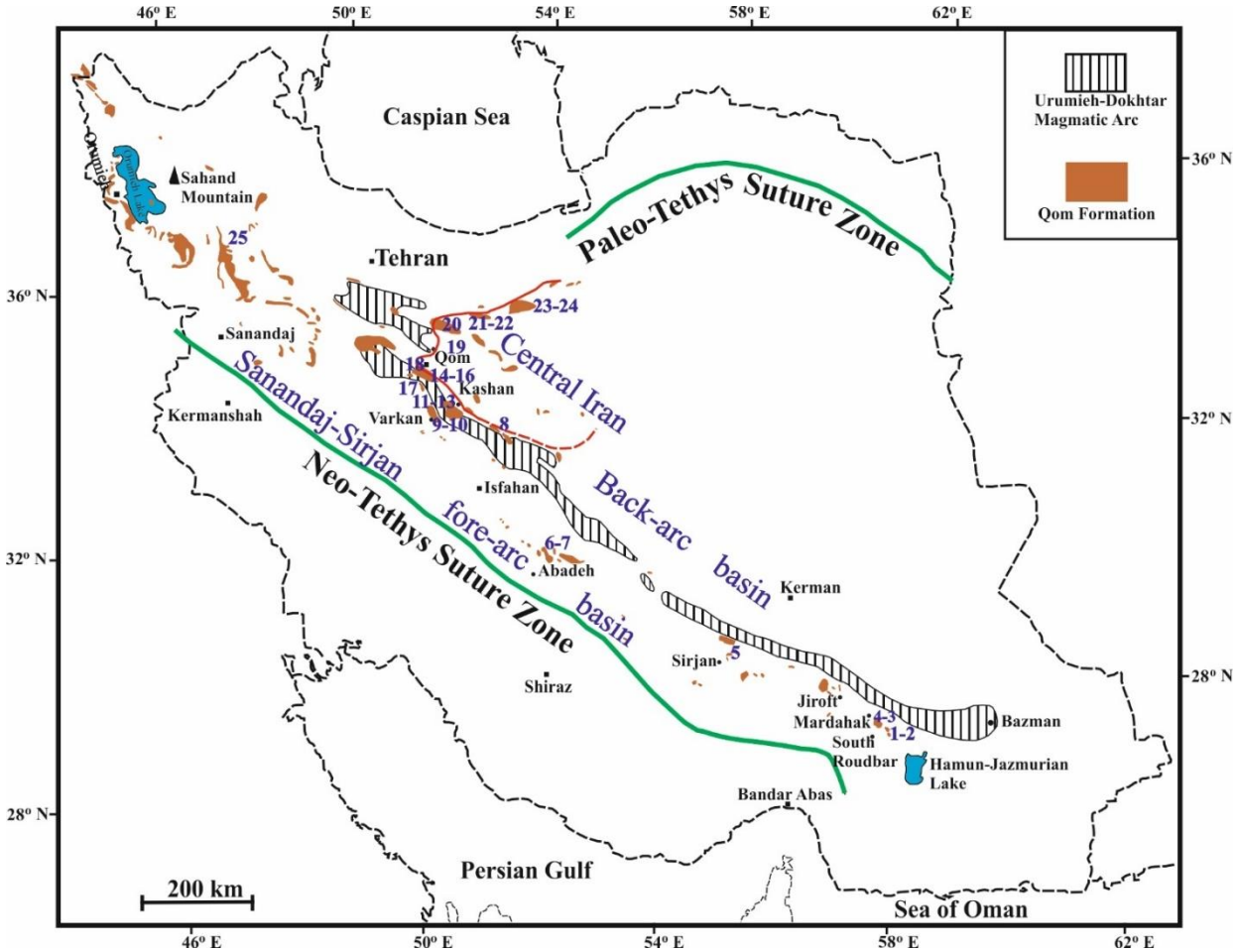

Fig 1- A map showing the distribution of Urumieh-Dokhtar Magmatic Arc, the Qom Formation outcrops, evaporite deposits (on the concave side of the red line), suture zones of Paleotethys and Neotethys in Iran, and the location of the study sections (after Mohammadi et al. 2013; Mohammadi 2023a)**. The stratigraphic sections containing rare microfacies are as follows: 1: Gonarestan; 2: Tavakolabad; 3: Bozdan; 4: Kegharaki; 5: Bujan; 6: Abadeh 1; 7: Abadeh 2; 8: Natanz; 9: Ghohroud; 10: Varkan; 11: Jazeh; 12: Vidoja; 13: Margh; 14: Shura; 15: Khurabad; 16: SE Qom** (Seddighi et al. 2011)**; 17: NE Delijan** (Karavan et al. 2015)**; 18: Qom area** (Okhravi and Amini 1998)**; 19: Alborz anticline Wells, NE Qom** (Rezaei et al. 2000)**; 20: S Tehran** (Jalali et al. 2017)**; 21: S Garmsar** (Jalali et al. 2016)**; 22: Deh Namak, NW Garmsar** (Daneshian et al. 2017)**; 23: Saran Section, SW Semnan** (Karami-Movahed et al. 2016)**; 24: Ghalibaf section, NW Semnan** (Sharifi et al. 2023)**; 25: Mianeh-Bostanabad area** (Bakhshi et al. 2015)**.**

Accordingly, the primary objective of this study is to provide the first regional synthesis of the rare microfacies of the Qom Formation by documenting their temporal and spatial distribution, depositional environments, and associated depositional models. The results contribute to a better understanding of the paleogeography of the Tethyan Seaway, as well as carbonate platform evolution and paleogeographic development during the Oligo–Miocene in Iran.

Methods

This study integrates original field observations with an extensive synthesis of previously published sedimentological and microfacies investigations in order to evaluate the temporal and spatial distribution of rare microfacies within the Qom Formation.

The first part of the study involved a comprehensive re-examination of microfacies data obtained from more than 15 stratigraphic sections previously investigated by the first author across different sectors of the Qom Basin (Gonarestan, Tavakolabad, Bozdan, Kegharaki, Bujan, Abadeh 1, Abadeh 2, Natanz, Ghohroud, Margh, Varkan, Jazeh, Vidoja, Shurab, Khurabad). The classification of carbonate rocks follows the schemes of Dunham (1962) and Embry and Klovan (1971). These original datasets were subsequently complemented by an exhaustive review of nearly all available peer-reviewed publications addressing the sedimentology, microfacies, depositional environments, and carbonate platform evolution of the Qom Formation. These articles include: Rahimzadeh (1994), FaizNia and Mosafi (1998), Okhravi and Amini (1998), Rezaei et al. (2000), Vaziri-Moghaddam and Torabi (2004), Seyrafian and Torabi (2005), Seyrafian et al. (2006), Khalili et al. (2007), Daneshian et al. (2008, 2010, 2017), Mohammadi et al. (2009, 2011, 2013, 2014, 2015, 2016, 2019, 2022), Mohammadi et al. (2009), Behforouzi et al. (2010), Dehghan et al. (2010), Seddighi et al. (2011), Mohammadian et al. (2013), Anjumshoa and Amirshahkarami (2014), Safari et al. (2014), Amirshahkarami and Karavan (2015), Bakhshi et al. (2015), Karavan et al. (2015), Mohammadi and Ameri (2015, 2017, 2018, 2024), Nouradini et al. (2015), Hoseini Nejad et al. (2016), Jalali et al. (2016, 2017), Karami-Movahed et al. (2016), Maghfori Moghadam et al. (2017), Holakouee et al. (2018), Mahyad et al. (2018, 2019), Noori et al. (2018), Asadi Mehmandosti et al. (2019), Aftabi Araniet et al. (2020, 2023), Hassanzadeh et al. (2020); Khaksar (2020), Mohammadi (2020a, 2020b, 2020c, 2021a, 2021b, 2021c, 2021d, 2023a, 2023b, 2024b, 2026), Rabbani et al. (2020), Safari et al. (2020a, 2020b), Navavajary et al. (2021), Noroozpour (2021), Rahiminejad et al. (2022), Lázár et al. (2023), Sharifi et al. (2023), Yazdi Moghadam et al. (2023), Mohammadi and Ghaedi (2024), Mohammadi and Sadeghi

https://doi.org/10.22108/jssr.2026.150537.1340

(2024), Piller et al. (2024), Sharifi-Yazdi et al. (2025), Sarkar et al. (2025), Kiani et al. (2026) and Ghaedi et al. (2026).

The photomicrographs and field photographs of the microfacies were selected from the original published sources, with the corresponding references provided. For rare microfacies for which the quality of the available images in the original sources was inadequate (Okhravi and Amini 1998; Bakhshi et al. 2015), or for which no microfacies images were provided (Rezaei et al. 2000), images were necessarily omitted. In some cases, although a microfacies was apparently reported as rare or infrequently occurring, its description, interpretation, or illustrated image was not consistent with the assigned microfacies designation. Such cases were therefore excluded from the list of rare microfacies.

Rare microfacies were identified not only on the basis of their assigned microfacies names but also through careful evaluation of their principal allochems, matrix composition, sedimentary textures, and diagnostic petrographic characteristics. This approach minimized inconsistencies arising from variations in microfacies nomenclature among different studies and provided a standardized basis for regional comparison.

For each identified rare microfacies, the corresponding depositional environment was reassessed using the sedimentological interpretations presented in the original publications together with accepted carbonate facies models. Particular attention was given to the depositional model proposed for each stratigraphic section in order to evaluate the relationship between rare microfacies occurrence and carbonate platform architecture.

The depositional interpretations presented here follow those provided in the original studies from which the microfacies were compiled, and no independent environmental interpretation is proposed by the authors. For some rare microfacies, the original studies do not provide an explicit depositional interpretation, although the corresponding depositional environment is identified. In such cases, we retain the environmental information and interpretive framework of the original study rather than introducing a new interpretation. Where necessary, the depositional setting is assigned on the basis of the associated microfacies assemblages characteristic of specific depositional sub-environments and the stratigraphic position of the microfacies within the corresponding depositional model.

To facilitate regional comparison, all investigated sections were arranged according to their geographic latitude, allowing spatial trends in microfacies distribution to be readily recognized. The compiled dataset includes geographic location, stratigraphic age, depositional environment, depositional model, and the principal petrographic characteristics of each rare microfacies. These data are summarized in Tables 1 and 2.

Representative photomicrographs of the identified rare microfacies were compiled from the original published sources, with full acknowledgement of the respective references, and are presented in Figs 2–4 to illustrate their principal petrographic features. In addition, rare petrofacies of the Qom Formation are summarized in Table 3.

Table 1- Summary of published records of rare microfacies of the Qom Formation, including study areas and stratigraphic boundaries.

row	Researcher(s)	Area/section	Lower and upper boundaries of the QF	Rare microfacies
1	Sharifi et al. 2023	Ghalibaf section, NW Semnan	Eocene rocks/ URF	RMF1a, RMF2, RMF7b, RMF8b, RMF8c, RMF8d, RMF10, RMF11a,
2	Karami-Movahed et al. 2016	Saran Section, SW Semnan	LRF/URF	RMF1b, RMF14b, RMF15a,
3	Bakhshi et al. 2015	Mianeh-Bostanabad area	Older rock with different ages/ URF	RMF3, RMF11c, RMF13a,
4	Okhravi and Amini (1998)	Qom area	LRF/URF	RMF4
5	Rezaei et al. 2000	Alborz anticline Wells, NE Qom	LRF	RMF11d
6	Mohammadi 2027	Bozdan section, SE Kerman	Eocene volcanic rocks/ Quaternary alluvium	RMF5,
7	Mohammadi and Sadeghi 2024	Shurab section, SE Qom	LRF/URF	RMF6,
8	Seddighi et al., 2011	SE Qom	B-Member and D-Member of the QF	RMF7a, MF8a,
9	Safari et al. (2014); Mohammadi (2021c)	Varkan, SW Kashan	LRF/ Pliocene polymictic conglomerate	RMF9, RMF5,
10	Jalali et al. 2016	S Garmsar	LRF/URF	RMF11b,
11	Ghaedi et al. 2026	SE Kerman, SW Kashan, NE Natanz	Different units	RMF12
12	Karavan et al. 2015	NE Delijan	LRF/ alluvium	RMF13b,
13	Aftabi Arani et al. 2020	Naraq area (NE Delijan)	LRF/ alluvium	RMF13c
14	Jalali et al. 2017	S Tehran	Eocene volcanic rocks	RMF14a,
15	FaizNia and Mosafi 1998	S Semnan	LRF/URF	RMF14c
16	Hosseininezhad et al. 2016	Talan Kuh Section, SW Semnan	LRF/ alluvium	RMF15b
17	Daneshian et al. 2017	Deh Namak, NW Garmsar	LRF/URF	RMF16

Result & discussion

Rare microfacies of the Qom Formation

Rare microfacies of the Qom Formation have been described and interpreted based on the data provided in the corresponding original references. The microfacies are generally presented in an order intended to reflect a progressive transition from deeper- to shallower-water depositional settings; however, this arrangement should not be regarded as strictly definitive. Rare microfacies are designated by the prefix “RMF”.

RMF1: Turbiditic microfacies

RMF1a: Graded bedding and Bouma sequence packstone with planktonic foraminifera (Ghalibaf section, NW Semnan; Sharifi et al. 2023)**:**

The microfacies is composed of light- to dark-grey limestones and is dominated by planktonic foraminifera, which account for approximately 50–60% of the allochems. Small benthic foraminifera, fragmented bivalve shells, and sponge spicules constitute the subordinate biotic constituents (Fig 2a–c). A distinctive feature of this microfacies is the coexistence of faunal elements indicative of both shallow-water conditions, represented mainly by small miliolids, and deeper-water settings, represented by planktonic foraminifera. Glauconite and opaque minerals are also present as minor components, collectively accounting for less than 1% of the grains.

Sedimentary structures and fabrics associated with gravity-flow deposition are also recognized in this microfacies. A fining-upward cycle corresponding to Unit A of the Bouma sequence can be identified (Fig 2a-c). Both intact and fragmented bioclastic components occur within the succession, with some grains exhibiting a preferred parallel orientation, suggesting post-depositional transport or reworking and corresponding to Unit B of the Bouma sequence. In addition, field observations document ripple lamination, which is interpreted as Unit C of the Bouma sequence (Fig 2a-c). This RMF was deposited in the lower part of the slope, below the storm wave base.

RMF1b: Calciturbidite (bioclastic benthic–planktonic foraminiferal wackestone–packstone) (Saran Section, SW Semnan; Karami-Movahed et al. 2016)**:**

This facies comprises wackestone to packstone textures and is distinguished by a mixed assemblage of benthic and planktonic biotic components (Fig 2d). The skeletal assemblage is dominated by fragmented coral and red algae debris, together with benthic foraminifera, particularly miliolids and Textularia, as well as planktonic foraminifera. Bivalve and echinoderm debris and peloid grains occur as additional constituents of the microfacies. The coexistence of shallow-water benthic elements with planktonic forms suggests deposition under marine conditions influenced by an open-water connection, while the wackestone–packstone texture indicates relatively low- to moderate-energy depositional conditions with variable degrees of bioclastic accumulation and reworking. The sudden changes in the basin slope, the presence of extensive barrier reef, the existence of calciturbidite and gravity sediments as well as the high proportion of grain-supported microfacies indicated that Qom Formation deposited on a shelf carbonate platform system (rimmed shelf).

RMF2: Breccia (Ghalibaf section, NW Semnan; Sharifi et al. 2023)**:**

The breccia beds display a predominantly clast-supported fabric and are composed of angular, polymictic clasts that differ lithologically from the enclosing host rock (Fig 2e-h). The individual clasts range from a few millimeters to several centimeters in size and exhibit mudstone as well as bioclastic packstone–grainstone textures. A conspicuous characteristic of these deposits is their highly chaotic internal fabric, reflecting the accumulation of poorly sorted intraformational fragments. The beds commonly possess sharp, erosional basal contacts and occur as laterally discontinuous, lenticular bodies.

These breccia intervals are intercalated with calciturbidites, locally associated with lens-shaped bodies and channelized geometries, suggesting deposition from sediment gravity flows within a slope setting. The combination of erosional bases, chaotic fabric, poor sorting, and channelized to lenticular architecture is consistent with episodic mass transport and gravity-flow processes. Overall, the breccia beds are interpreted to have accumulated along the lower part of the slope, below the storm wave base, where storm-generated reworking was limited and downslope sediment transport and gravity-driven deposition became the dominant processes.

RMF3: Sandy planktonic Foraminifera wackestone- Silty planktonic foraminifera mudstone (Mianeh-Bostanabad area; Bakhshi et al. 2015):

This microfacies association is characterized by planktonic foraminifera dispersed within a micritic to fine-grained groundmass, accompanied by echinoderm fragments and other bioclastic debris. Detrital quartz, ranging from fine- to medium-grained sand size and locally accounting for approximately 20% of the framework constituents, is a prominent component of the sandy variety, whereas the silty variety is characterized by a finer-grained groundmass and sparse planktonic foraminifera. In some beds, the "sandy planktonic foraminiferal wackestone" gradually passes into "silty planktonic foraminiferal mudstone", reflecting a decrease in grain size and siliciclastic input. Iron oxides locally occur within foraminiferal chambers and as a cementing phase as a result of diagenetic alteration.

The occurrence of planktonic foraminifera, together with the fine-grained texture and siliciclastic input, is consistent with deposition along the distal middle-ramp to slope transition, where marine currents and turbidity currents influenced sediment accumulation.

RMF4: bioturbated, bioclastic wackestone (with planktonic foraminifera and coralline algae) (Qom area; Okhravi and Amini 1998):

This RMF is represented by medium-bedded, greenish-grey to cream-coloured, fine-grained argillaceous limestone. It consists of a bioturbated, bioclastic wackestone with a carbonate-rich groundmass containing particles up to silt size. Planktonic foraminifers and fragments of coralline algae, averaging approximately 0.33 mm in diameter, are the principal components, whereas particles derived from benthic biota are relatively scarce. Volcanic quartz and feldspar grains are common, and some samples locally grade into tuffaceous limestone.

The predominance of planktonic foraminifera, together with reef-derived coralline algae fragments, points to deposition along the outer slope to basin transition. Seaward, this microfacies grades into grey pelagic marl of the e-Member, representing the deepest-water deposits.

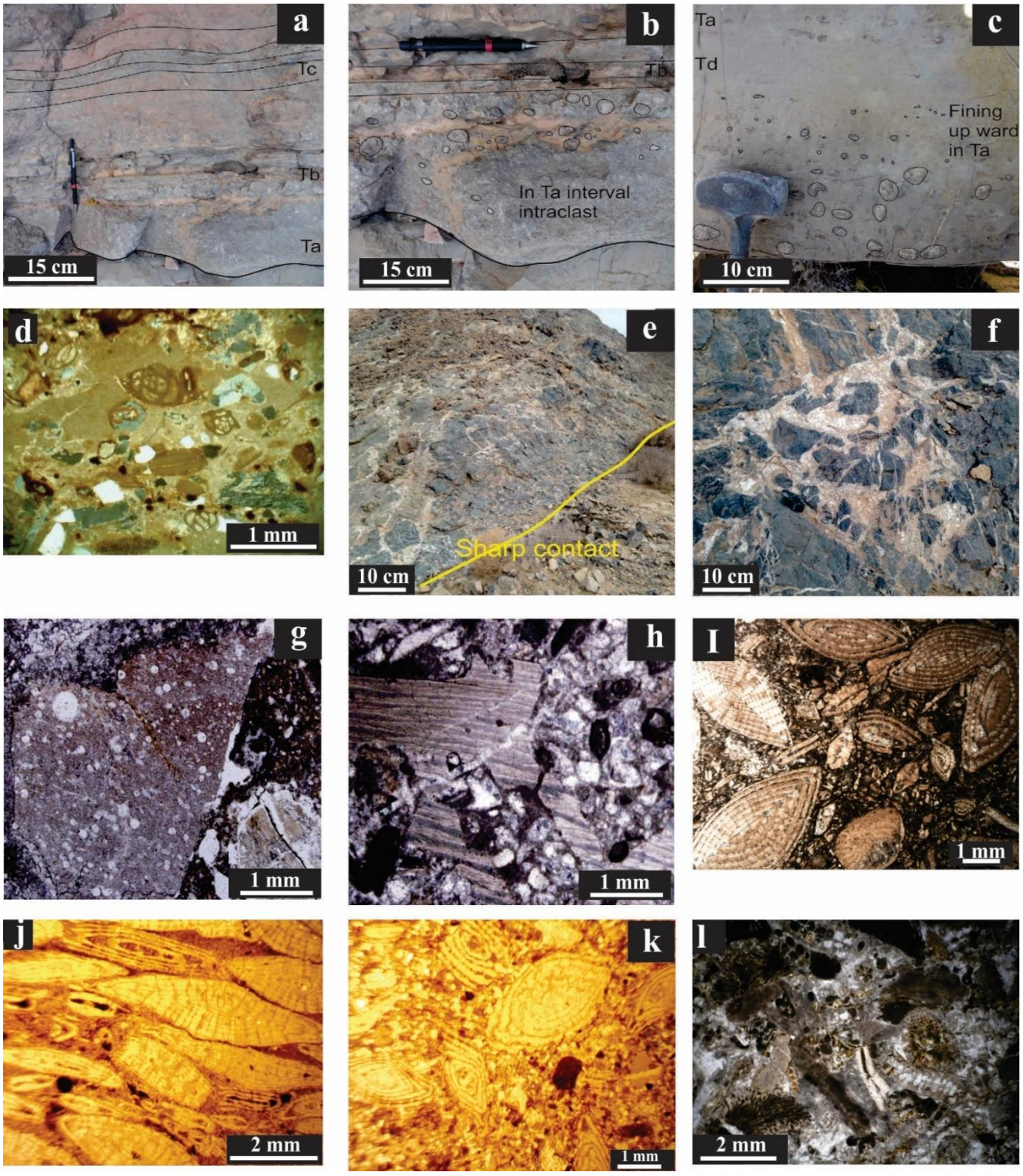

Fig 2- Field photographs and photomicrographs of the rare microfacies of the Qom Formation: a-b) Field photograph of RMF1a: graded bedding and Bouma sequence packstone with planktonic foraminifera, showing an erosional base; a, b: graded bedding; c: incomplete Bouma sequence (Bouma 1962; Sharifi et al. 2023)**; d) RMF1b: Calciturbidite (bioclastic benthic–planktonic foraminiferal wackestone–packstone;** Karami-Movahed et al. 2016)**; e-h) Field and photomicrographs of RMF2: breccia; g and h show grey breccia with angular clasts** (Sharifi et al. 2023)**; i-k) RMF5a: *Nummulites* packstone; i: Bujan section; J-k: Bozdan section** (Mohammadi 2027; Mohammadi 2021c; Mohammadi et al. 2014)**; l) RMF6: Perforate foraminifera bryozoan, echinid packstone** (Mohammadi and Sadeghi 2024)**. Ta: Unit a of the Bouma sequence; Tb: Unit b of the Bouma sequence.**

RMF5: Nummulitid bearing microfacies

RMF5a: *Nummulites* packstone (Bozdan section, SE Kerman; Mohammadi 2027; Bujan section, Mohammadi et al. 2014):

This microfacies is characterized by abundant, predominantly intact and well-preserved, elongated *Nummulites*, with rotaliid small benthic foraminifera and echinoids occurring as subordinate components (Fig 2i-j).

https://doi.org/10.22108/jssr.2026.150537.1340

The assemblage and preservation state are consistent with deposition on the distal middle ramp, near the lower limit of the photic zone (Bassi et al. 2007; Brandano et al. 2009). Locally, the microfacies grades into a sandy Nummulites packstone (Fig 2k), reflecting the incorporation of quartz grains and/or tuffaceous-derived mineral grains into the carbonate sediment (Mohammadi 2027; Bozdan Section, SE Kerman).

RMF5b: *Operculina/ Heterostegina* packstone (Bujan section, SE Kerman; Mohammadi 2021c; Mohammadi et al. 2014):
This microfacies is dominated by *Operculina* and/or *Heterostegina*, which constitute the principal skeletal components. The tests are generally elongated, well preserved, and commonly occur intact, indicating limited post-mortem transport and mechanical reworking (Fig 3a-b).

The widespread occurrence of hyaline-walled foraminifera, coupled with the absence of imperforate (porcellaneous) forms, is indicative of normal marine salinity (Hottinger 1983, 1997; Pomar 2001; Brandano et al. 2009). The abundance of well-preserved, hyaline-walled larger benthic foraminifera suggests deposition within the lower part of the photic zone under relatively calm conditions, below significant wave influence (Hottinger 1983, 1997; Pomar 2001; Romero et al. 2002). Accordingly, this microfacies is interpreted to have accumulated in an open-marine setting, within the mesophotic- oligophotic zone and under low- to moderate-energy hydrodynamic conditions.

RMF6: Perforate foraminifera bryozoan, echinid packstone (Shurab section, SE Qom; Mohammadi and Sadeghi 2024)**:**
This microfacies is distinguished by an assemblage of perforate foraminifera accompanied by abundant bioclasts. The larger foraminiferal assemblage comprises *Operculina*, *Heterostegina*, *Amphistegina*, and *Neorotalia*, whereas bryozoan and echinoid fragments constitute the principal bioclasts (Fig 2l).

Flatter, thinner test walls tend to occur with reduced light, with increasing water depth or turbidity (Beavington-Penney and Racey 2004; BouDagher-Fadel 2018). Operculina can occur in medium light conditions in a somewhat deeper part of the photic zone (Bassi et al. 2007; Sarkar et al. 2016). Heterotrophic organisms, such as bryozoans, are independent of light and water depth. therefore, they are capable of living in sub euphotic waters (Pomar 2001; Brandano and Corda 2002). The faunal assemblage and microfacies characteristics indicate deposition under low-energy conditions within the distal middle ramp, near the lower part of the photic zone.

RMF7: Coral-bearing microfacies
RMF7a: Coral rudstone (SE Qom: Seddighi et al. 2011)**:**
Coral fragments constitute the dominant component of this microfacies, which is characterized by a rudstone fabric containing abundant, highly fragmented and abraded coarse skeletal debris. The microfacies has a restricted distribution within the studied section.

Unlike in-place reef facies, this microfacies is marked by abundant angular coral fragments and lacks any preserved in-place boundstone fabric. The microfacies is interpreted to represent deposition on the proximal middle shelf, where coral-derived skeletal debris accumulated following fragmentation and limited transport.

RMF7b: Coral framestone (Ghalibaf section, NW Semnan; Sharifi et al. 2023):
This microfacies is represented by massive to thick-bedded, dome-shaped, dark-grey to cream-coloured limestones. Corals form the principal component and are commonly associated with calcite cement, whereas bivalves and benthic foraminifera occur as subordinate constituents. Minor amounts of fine sand-sized quartz grains are also present. The corals developed a laterally continuous framework that can be traced over considerable distances (Fig 3d-e), indicating an established in-place reef structure. Accordingly, this microfacies is interpreted to represent a reef environment, particularly barrier reefs developed along rimmed-carbonate platform margins.

RMF8: Intraclast-bearing microfacies:
RMF8a: Intraclast, bryozoa bioclast grainstone (SE Qom: Seddighi et al. 2011)**:**
This microfacies is composed mainly of bryozoa, corallinacean red algae, echinoid fragments, and bivalve shell debris, accompanied by benthic foraminifera, including *Miogypsina* and *Elphidium*, and intraclasts. The grains are poorly sorted and range in size from medium- to coarse-grained sand to granule (Fig 3c).

The grain-supported texture and abundance of fragmented skeletal components point to deposition under relatively high-energy conditions, probably near the fair-weather wave base (FWWB; Flügel 2010).

RMF8b: Intraclast bioclastic rudstone-floatstone (Ghalibaf section, NW Semnan; Sharifi et al. 2023)**:**
This microfacies consists of dark-grey, medium-bedded limestones displaying a floatstone–rudstone alternation. The beds are commonly graded and contain a diverse skeletal assemblage of brachiopods, crinoids, bivalves, echinoids, benthic foraminifera, calcareous red algae, and corals. The rudstone–floatstone intervals are characterized by abundant intraclasts and allochems, with poorly sorted fragments ranging from sub-rounded to irregular in outline and approximately 2–3 mm in size. Graded bedding and erosional bases constitute the main sedimentary structures (Fig 3f), while the skeletal and intraclast components are dispersed within a combination of sparry calcite cement and micritic matrix.

RMF8c: Intraclastic bioclastic grainstone- rudstone (Ghalibaf section, NW Semnan; Sharifi et al. 2023)**:**
This microfacies is represented by grey to dark-grey, thick-bedded limestone containing relatively well-sorted grains. A characteristic feature is a coarsening-upward trend, locally accompanied by rare cross-lamination and massive bedding. The skeletal and non-skeletal assemblage is dominated by bioclastic components, including echinoids, brachiopods, red algae, and bivalves, together with intraclastic fragments. The grains are generally well sorted, whereas the micritic matrix has been largely removed and subsequently occluded by sparry calcite cement (Fig 3g-h).

RMF8d: Intraclastic grainstone (Ghalibaf section, NW Semnan; Sharifi et al. 2023)**:**
This microfacies is characterized by thin-bedded, dark-grey limestones with an orthochem-rich fabric and moderate to good sorting of coarse- to medium-grained particles. Sub-rounded, well-sorted intraclasts constitute the principal non-skeletal components of the microfacies (Fig 3I). Skeletal material is relatively minor, occurring mainly as small fragments of bivalves and echinoids.

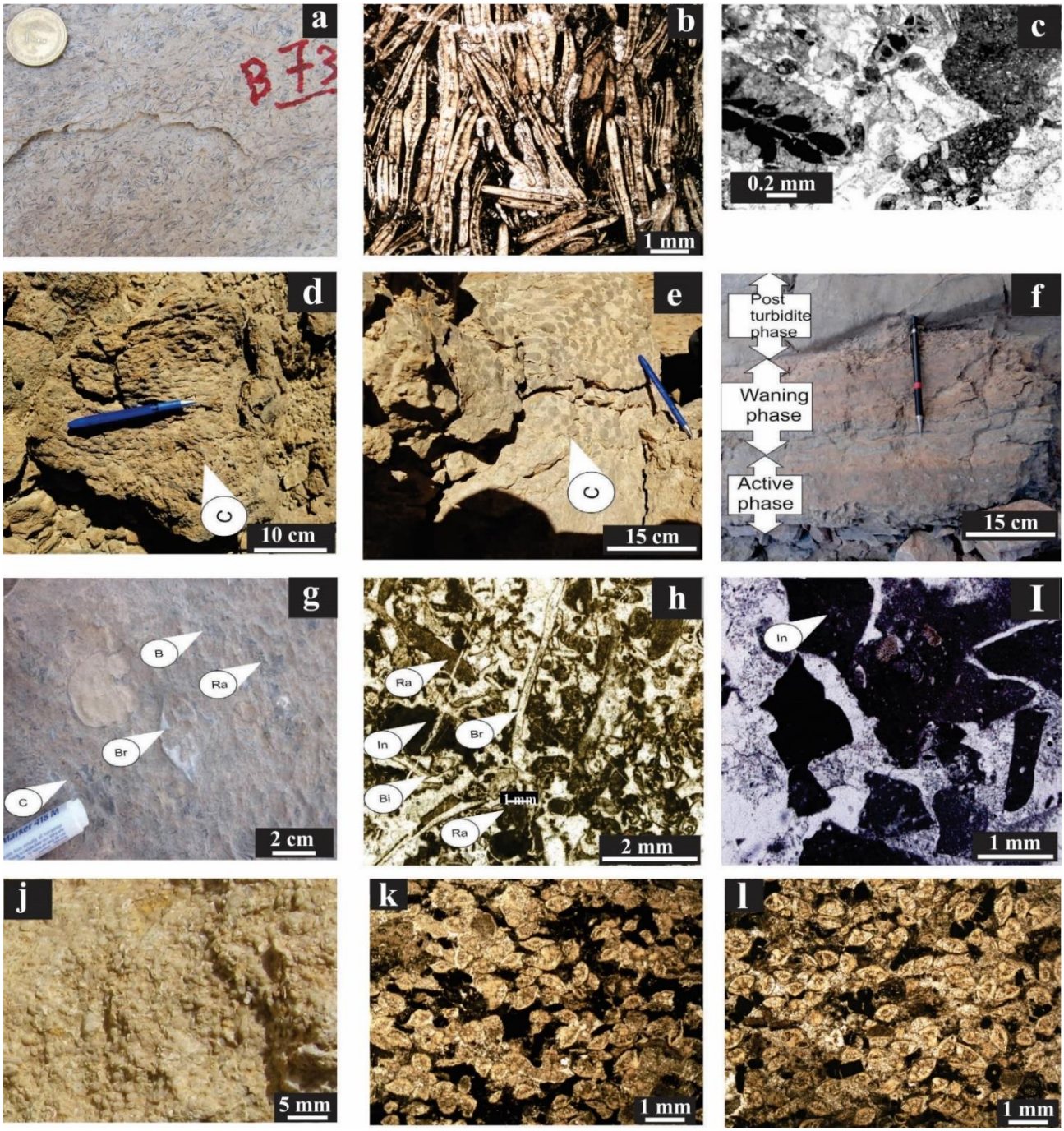

Fig 3- Field photographs and photomicrographs of the rare microfacies of the Qom Formation: a-b) Field photographs and photomicrographs of RMF5b: *Operculina*/ *Heterostegina* packstone (Mohammadi 2021c; Mohammadi et al. 2014)**; c) RMF8a: Intraclast, bryozoa bioclast grainstone** (Seddighi et al. 2011)**; d and e) Field photograph of RMF7b: Coral framestone. Corals occur as patch reef,** (Sharifi et al. 2023)**; f) Field photograph of RMF8b: intraclast bioclastic rudstone-floatstone microfacies in the Bouma sequence** (Sharifi et al. 2023)**; g and h) Field photographs and photomicrographs of RMF8c: intraclastic bioclastic grainstone-rudstone, the space between the grains is filled by calcite cement** (Sharifi et al. 2023)**; i) Photomicrograph of RMF10: intraclastic grainstone** (Sharifi et al. 2023)**; j-l) Field photographs and photomicrographs of RMF9: *Neorotalia* packstone** (Safari et al. 2014; Mohammadi 2021c)**. Cr: crinoid; C: coral; Ra: red algae; E: echinoid; Br: brachiopod; In: intraclast; B: bryozoan; Bi: bioclast.**

RMF9: *Neorotalia* packstone (Varkan, SW Kashan; Safari et al. 2014; Mohammadi 2021c; Mohammadi 2023b)**:**
This microfacies is overwhelmingly dominated by *Neorotalia*, particularly *N. viennoti*, which locally occurs in rock-forming abundance (Fig 3j-l).

Modern tropical carbonates commonly contain calcarinid beach sands and shoal sands (Hallock 1984), suggesting that this microfacies may represent a shoal deposit or downslope reworking of material derived from a shoal. The size-sorted *Neorotalia* tests, together with their limited abrasion, indicate relatively short-distance transport, whereas the angular morphology of the mudstone intraclasts likewise suggests

https://doi.org/10.22108/jssr.2026.150537.1340

limited reworking. A predominantly sparry groundmass further supports deposition in a relatively high-energy, shoal-type environment (Safari et al. 2014; Mohammadi 2021c; Varkan SW Kashan).

RMF10: Crinoid grainstone (Ghalibaf section, NW Semnan; Sharifi et al. 2023)**:**
This microfacies consists of grey, thick-bedded limestone characterized by relatively well-sorted grains. Crinoid and echinoid tests are overwhelmingly dominant among the skeletal components (Fig 4a-b), whereas brachiopod and bivalve fragments occur as subordinate constituents. The skeletal-rich, grain-supported character is consistent with deposition on platform-margin sand shoals and bars within the photic zone and above the fair-weather wave base (FWWB) (Wilson 1975).

RMF11: Ooid-bearing microfacies
RMF11a: Bioclastic ooidal grainstone (Ghalibaf section, NW Semnan; Sharifi et al. 2023)**:**
This microfacies is represented by cream-colored, massive to thick-bedded limestones displaying parallel bedding (Fig 4c-d). Ooids constitute the dominant allochems, with cement locally occluding the interparticle porosity. The skeletal allochems are mainly represented by miliolids and bivalves. Composite ooids are also present, commonly containing brachiopod and echinoid tests as their nuclei (Fig 6K). The ooid-rich, grain-supported character is consistent with deposition on platform-margin sand shoals and bars within the photic zone and above the FWWB (Flügel 2010).

RMF11b: Oolitic Grainstone – Packstone (East Siyah Kuh surface section, S Garmsar; Jalali et al. 2016):
Ooids constitute the most abundant non-skeletal allochems in this microfacies and are associated with skeletal components including echinoids, red algae, miliolids, ostracods, gastropods, bryozoans, and larger imperforate foraminifera, whose occurrence varies according to their position within the depositional setting. The ooids are predominantly about 200 µm to 1 mm in diameter and are mainly represented by normal ooids (Type 1 ooids) characterized by a single cortical lamina (Flügel 2010). Pseudo-ooids are also locally observed in some samples. Cross-bedding is among the principal sedimentary structures developed within this microfacies. Dissolution is the dominant diagenetic process affecting this microfacies. Most ooid nuclei, together with some ooid grains and skeletal allochems such as gastropods and bivalves, have undergone selective dissolution, resulting in the development of abundant moldic porosity. Consequently, porosity locally reaches as much as 30%, making this microfacies one of the most prospective reservoir facies within the studied succession.

Based on its microfacies position, grain composition, and biotic assemblage, this microfacies is interpreted to have formed in a high-energy shoal setting, where persistent water agitation and sediment reworking promoted the development and accumulation of ooidal grain-rich sediments.

RMF11c: Sandy ooid packstone (Yengeh-Jeh section, Mianeh-Bostanabad area; Bakhshi et al. 2015):
This microfacies is characterized by an ooid-rich packstone containing abundant siliciclastic detritus, including fine- to medium-grained quartz, feldspar, and lithic fragments. The nuclei of the ooids are predominantly composed of sand-sized quartz grains. Scattered bioclasts, including bivalve and bryozoan fragments, are also present within the microfacies. The micritic matrix is subordinate and occurs in only minor amounts. The distribution of this microfacies is limited, being recognized only in the Yengejeh stratigraphic section. It was deposited in the tidal zone (Wilson 1975; Flügel 2010).

RMF11d: Ooid Grainstone (Alborz anticline wells, NE Qom; Rezaei et al. 2000)
This microfacies is characterized by a grainstone texture, with ooids constituting the principal allochems. Most of the ooids have undergone dissolution, apparently as a result of exposure to meteoric waters undersaturated with respect to calcium carbonate, producing secondary oomoldic porosity. The cement includes isopachous calcite cement, syntaxial calcite overgrowths, drusy calcite cement, and pervasive gypsum cement.

The abundance of ooids, together with the grain-supported fabric, indicates deposition in a shallow, high-energy, agitated oolitic shoal environment (Flügel 2010).

RMF12: Gastrochaenolites-bearing microfacies (Varkan, Bujan, Gonarestan, and Natanz sections; Mohammadi 2020b; Mohammadi 2021c; Mohammadi and Ghaedi 2024; Ghaedi et al. 2026):
This microfacies is characterized by the presence of *Gastrochaenolites* (Fig 4e-h). *Gastrochaenolites* is a clavate boring produced primarily by endolithic bivalves within lithic substrates (Ghaedi et al. 2026). Its occurrence is indicative of moderate to high hydrodynamic energy, oligotrophic to slightly mesotrophic nutrient regimes, and shallow euphotic depths, ranging from intertidal settings to a few meters below the low-tide level (Mohammadi and Ghaedi 2024; Ghaedi et al. 2026). Based on the occurrence of *Gastrochaenolites*, the associated biota, and its stratigraphic position, the *Gastrochaenolites*-bearing microfacies of the Qom Formation is interpreted to have been deposited in a shallow, restricted lagoon under moderate to high hydrodynamic energy.

RMF13: Peloid-bearing microfacies
RMF13a: Peloid packstone (Mianeh-Bostanabad area; Bakhshi et al. 2015):
This microfacies is characterized as a red algal peloid packstone. Peloids constitute the dominant component of the microfacies, whereas red algae, bivalve fragments, and miliolids represent subordinate skeletal and biogenic constituents. This microfacies was deposited in a lagoon.

RMF13b: Imperforate Foraminiferal–Peloidal Packstone–Grainstone (NE Delijan; Karavan et al. 2015):
This microfacies is characterized by abundant imperforate benthic foraminifera, including miliolids, *Borelis*, and *Peneroplis*, which collectively account for approximately 43% of the allochems. Skeletal debris, comprising echinoderm fragments, bivalves (ostrea), coralline algae, gastropods, and bryozoans, constitutes a further 10% of the microfacies (Fig 4i). The skeletal components are predominantly fragmented, although locally intact specimens are also preserved within the groundmass. Peloids are relatively abundant, accounting for approximately 25% of the allochems. Interparticle pore spaces are commonly occluded by sparry calcite cement, occurring mainly as granular to blocky crystals. In the field, this microfacies is typically expressed as thin- to medium-bedded grey to buff-coloured calcylutite and thin-bedded greenish marly limestone. Micritization and hematitization are locally developed within some carbonate grains.

The association of imperforate foraminifera, particularly miliolids, *Borelis*, and *Peneroplis*, together with abundant peloids and a micritic matrix, indicates deposition in a low-

energy lagoonal setting (Geel 2000; Flügel 2010).

RMF13c: Bioclastic–peloidal packstone/wackestone (Naraq area, NE Delijan; Aftabi Arani et al. 2020):

This microfacies comprises packstone to wackestone containing abundant bioclasts and peloids. Red algal fragments, both intact and reworked, constitute the dominant skeletal component. Ostracods, bryozoans, bivalves, corals, echinoderms, and lagoonal foraminifers such as Quinqueloculina, Massilina, Pyrgo, Borelis, and Spiroloculina, together with shallow-marine hyaline foraminifers such as Rotalia, are also present. Peloids constitute the main non-skeletal component and locally exceed 10% of the rock fabric. The abundance of fragmented reef-building organisms, particularly red algae and bryozoans, together with fecal pellets and a diverse skeletal assemblage, is consistent with deposition in a shallow inner-platform setting adjacent to a reef, probably within an open lagoon.

RMF14: Ostracod-bearing microfacies

RMF14a: Bioclastic Ostracoda Mudstone – Wackestone (Yort e Shah No-1 well and Morreh Kuh surface section, S Tehran; Jalali et al. 2017):

The microfacies is composed predominantly of ostracods (up to 15%), miliolids (up to 5%), gastropods, red algae, ammonoids, and echinoids, which are sparsely distributed within a micritic matrix. The replacement of skeletal grains, particularly ostracods, and the matrix by gypsum, together with dolomitization and the development of fenestral fabric (Fig 4j), represent the principal diagenetic features observed in this microfacies. Minor amounts of siliciclastic detritus, ranging from silt- to very fine sand-size, occur locally and account for approximately 1–4% of the microfacies.

The occurrence of fenestral fabric, together with the low biotic diversity, suggests deposition under low-energy conditions within the inner-ramp (restricted lagoon) to intertidal domain (Alsharhan, and Kendall 2002; Rasser et al. 2005). This interpretation is consistent with shallow, restricted depositional settings characterized by episodic subaerial exposure and limited water circulation.

RMF14b: Gastropoda ostracods bioclast grainstone (Saran Section, SW Semnan; Karami-Movahed et al. 2016)**:**

Shell fragments, ostracods, gastropods, and benthic foraminifera, particularly miliolids, constitute the principal allochems of this microfacies. Peloids and intraclasts occur as minor components, dispersed within a sparry calcite cement (Fig 8C). The abundance of coarse skeletal particles, especially gastropods, bivalves, and ostracods, together with their association with sparry calcite cement and the scarcity of open-marine fauna, points to deposition in a relatively high-energy tidal environment, specifically within the subtidal zone. This sub-environment likely represented tidal-flat channels connecting the lagoonal domain with the adjacent tidal-flat area.

RMF14c: Ostracod lime wackestone (S Semnan; FaizNia and Mosafi 1998)**:**

This microfacies is characterized by ostracod remains accompanied by fragments of gastropod and/or bivalve shells embedded in a micritic matrix, with other skeletal components being absent. The presence of evaporitic minerals, together with the restricted skeletal assemblage, was interpreted as indicative of a low-energy, intertidal setting. It is noteworthy that shallow epicontinental seas have been proposed as the depositional setting for the Qom Formation in the study area.

RMF15a: Fenestral mudstone (Saran Section, SW Semnan; Karami-Movahed et al. 2016)**:**

This microfacies consists predominantly of marl and mudstone, with fossil and bioclastic particles generally accounting for less than 10% of the rock fabric. The most distinctive feature of this fine-grained microfacies is the development of bird's-eye (fenestral) fabric. Locally, silt-sized detrital quartz grains are also present (Fig 4k), whereas the matrix is largely composed of microcrystalline clay. The very low abundance of grains reflects deposition under calm, low-energy conditions with limited wave agitation. The bird's-eye fabric is commonly attributed to the entrapment of gas bubbles associated with foam formation along the shoreline, as well as organic-matter decay and algal photosynthesis within the sediment (Flügel 2010). Together with the scarcity of bioclasts, its well-developed fenestral fabric indicates a position close to the landward margin of the depositional system. Accordingly, this microfacies is interpreted as representing a tidal to intertidal, locally supratidal environment (Karami-Movahed et al. 2016; Saran Section, southwestern Semnan).

RMF15b: Fenestral mudstone (Talan Kuh Section, SW Semnan; Hosseininezhad et al. 2016)**:**

This microfacies consists of fossil-free micrite characterized by a distinct fenestral fabric. The absence of skeletal components and the development of fenestrae are consistent with deposition in an intertidal setting.

RMF16: Stromatolites Bindstone (Deh Namak, NW Garmsar; Daneshian et al. 2017):

This microfacies is characterized by an alternation of dark- and light-colored laminae, consisting predominantly of micrite and mixed micrite–sparite layers (Fig 4l). Bird's-eye fenestrae are locally developed within the microfacies.

The occurrence of stromatolitic fabric in association with bird's-eye fenestrae is indicative of deposition in a tidal-flat setting characterized by variable energy conditions, ranging from relatively low- to locally higher-energy environments. Accordingly, this microfacies is interpreted as belonging to Facies Zone 9.

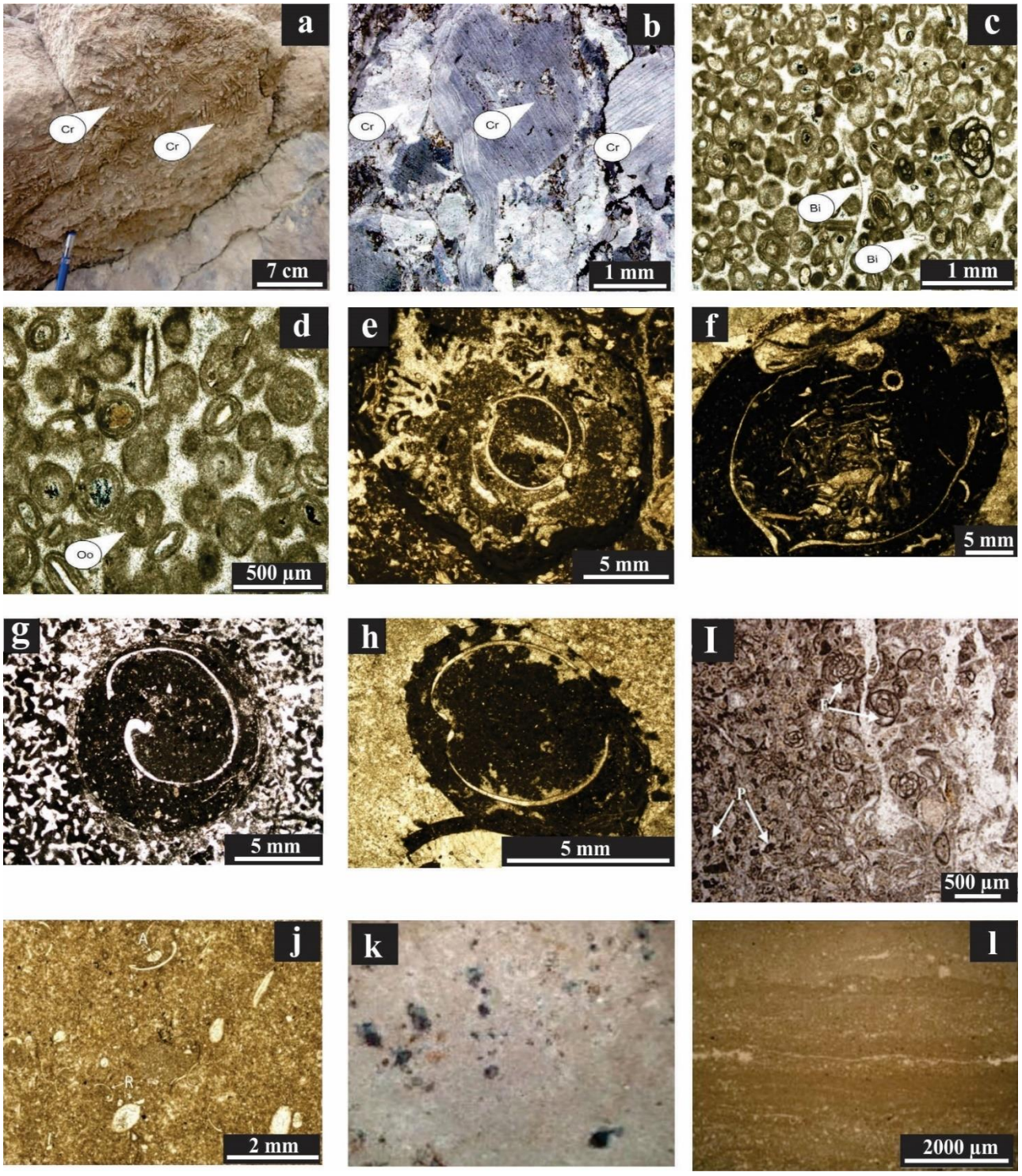

Fig 4- Field photographs and photomicrographs of the rare microfacies of the Qom Formation. a and b) Field photographs and photomicrographs of RMF10: crinoid grainstone, in which crinoids are the major component (Sharifi et al. 2023)**; c and d) Photomicrographs of RMF11a: bioclastic ooidal grainstone; allochems consist of ooids and bivalves, with the space between them filled with calcite cement; e-h) RMF12: Photomicrographs of Gastrochaenolites-bearing microfacies** (Mohammadi 2020b; Mohammadi 2021c; Mohammadi and Ghaedi 2024; Ghaedi 2026)**; i) Photomicrographs of RMF13b: Imperforate Foraminiferal–Peloidal Packstone–Grainstone** (Karavan et al. 2015)**; j) Photomicrographs of RMF14a: Bioclastic Ostracoda Mudstone – Wackestone** (Jalali et al. 2017)**; k) RMF15: Fenestral mudstone** (Karami-Movahed et al. 2016)**; l) Photomicrographs of RMF16: Stromatolites Bindstone** (Daneshian et al. 2017)**. Cr: crinoid; E: echinoid; Oo: ooid; Bi: bioclast.**

Table 2- Rare and distinctive microfacies of the Qom Formation and their depositional settings, locations, and ages.

Microfacies group	microfacies /sub- microfacies name	Depositional setting(s)	location	age
Turbiditic microfacies	RMF1a: Graded bedding and Bouma sequence packstone with planktonic foraminifera	lower slope part below the storm wave base	Ghalibaf section, NW Semnan	Early-Miocene
	RMF1b: Calciturbidite (bioclastic benthic–planktonic foraminiferal wackestone–packstone)	Open Marine (middle-outer ramp)	Saran Section, SW Semnan	Early-Miocene
	RMF2: Breccia	lower part of the slope, below the storm wave base	Ghalibaf section, NW Semnan	Early-Miocene
	RMF3: Sandy planktonic Foraminifera wackestone (Silty planktonic Foraminifera mudstone)	distal middle ramp	Mianeh-Bostanabad area	Early-Miocene
	RMF4: bioturbated, bioclastic wackestone (with planktonic foraminifera and coralline algae)	outer slope to basin	Qom area	Early-Miocene
Nummulitid packstone	RMF5a: *Nummulites* packstone	distal middle ramp, near the lower limit of the photic zone	Bozdan section, SE Kerman	Rupelian
	RMF5b: *Operculina*/ *Heterostegina* packstone	distal middle ramp	Bujan section, SE Kerman	Chattian
	RMF6: Perforate foraminifera bryozoan, echinid packstone	distal middle ramp, lower part of the photic zone	Shurab section, SE Qom	Oligocene
Coral-bearing facies	RMF7a: Coral rudstone	proximal middle shelf	SE Qom	
	RMF7b: Coral framestone	reef environment, particularly barrier reefs	Ghalibaf section, NW Semnan	Early-Miocene
Intraclast-bearing microfacies	RMF8a: Intraclast, bryozoa bioclast grainstone	relatively high-energy conditions, probably near the fair-weather wave base	SE Qom	?Aquitanian
	RMF8b: Intraclast bioclastic rudstone-floatstone	Upper slope	Ghalibaf section, NW Semnan	Early-Miocene
	RMF8c: Intraclastic bioclastic grainstone- rudstone	Platform-margin sand shoal	Ghalibaf section, NW Semnan	Early-Miocene
	RMF8d: Intraclastic grainstone	Platform-margin sand shoal	Ghalibaf section, NW Semnan	Early-Miocene
	RMF9: *Neorotalia* packstone	relatively high-energy, shoal-type environment	Varkan, SW Kashan	Rupelian
	RMF10: Crinoid grainstone	platform-margin sand shoals and bars	Ghalibaf section, NW Semnan	Early-Miocene
Ooid-bearing microfacies	RMF11a: Bioclastic ooidal grainstone	platform-margin sand shoals and bars	Ghalibaf section, NW Semnan	Early-Miocene
	RMF11b: Oolitic Grainstone – Packstone	high-energy shoal/ Barrier setting	East Siyah Kuh surface section, S Garmsar	Early-Miocene
	RMF11c: Sandy ooid packstone	tidal zone	Yengeh-Jeh section, Mianeh-Bostanabad area	Early-Miocene
	RMF11d: Ooide Grainstone	oolitic shoal environment	Alborz anticline, NE Qom	-
	RMF12: Gastrochaenolites-bearing microfacies	shallow, restricted lagoon with moderate to high hydrodynamic energy	Varkan, Bujan, Gonarestan, and Natanz sections	Oligocene
Peloid-bearing microfacies	RMF13a: Peloid packstone	Lagoon	Mianeh-Bostanabad area	Early-Miocene
	RMF13b: Imperforate Foraminiferal–Peloidal Packstone–Grainstone	low-energy lagoonal setting	NE Delijan	Rupelian-Chattian
	RMF13c: Bioclastic– peloidal packstone/ wackestone	open lagoon	NE Delijan	Aquitanian
Ostracod-bearing microfacies	RMF14a: Bioclastic Ostracoda Mudstone – Wackestone	restricted lagoon to intertidal settings characterized by episodic subaerial exposure and limited water circulation	Yort e Shah no-1 well and Morreh Kuh surface section, S Tehran	Early-Miocene
	RMF14b: Gastropoda ostracods bioclast grainstone	tidal flat channels	Saran Section, SW Semnan	Early-Miocene
	RMF14c: Ostracod lime wackestone	low-energy, intertidal setting	S Semnan	Early-Miocene
	RMF15: Fenestral mudstone	tidal to intertidal, locally supratidal environment	Saran Section, SW Semnan	Early-Miocene
	RMF15b: Fenestral mudstone	intertidal setting	Talan Kuh Section, SW Semnan	Early-Miocene
	RMF16: Stromatolites Bindstone	tidal-flat setting	Deh Namak, NW Garmsar	Early-Miocene

https://doi.org/10.22108/jssr.2026.150537.1340

Rare petrofacies of the Qom Formation

Although the number of detailed studies devoted to the non-carbonate petrofacies of the Qom Formation is relatively limited, the documented diversity, spatial distribution, and reported occurrence of these petrofacies are considerable. For example, Mohammadi (2021a) provided a relatively comprehensive list of more than 100 stratigraphic sections in which siliciclastic petrofacies, including conglomeratic, sandy, or mixed conglomeratic–sandstone facies, have been reported. Thus, despite the limited number of studies that have specifically focused on the detailed description of conglomeratic and sandstone facies, their documented occurrence and broad distribution suggest that these petrofacies may not readily be regarded as rare.

A similar consideration applies to the evaporitic petrofacies. Although detailed petrographic studies of evaporitic facies are even less numerous than those dealing with siliciclastic petrofacies, Mohammadi et al. (2013) demonstrated that evaporitic deposits of the Qom Formation are distributed over a substantial area of the Qom back-arc basin. According to Mohammadi et al. (2013), evaporite deposition occurred along the concave side of an assumed curved line extending from southeastern Anarak through Nain, the Navab Anticline southeast of Kashan, Shourab southeast of Qom, the areas immediately south, southwest, and west of Qom, north of Lake Howz Soltan, southwest of Tehran, southwest, west, and southeast of Varamin, northeast of Garmsar, and northwestern, northern, and northeastern Semnan (Fig 1).

Volcaniclastic petrofacies have received even less attention than the evaporitic facies, and Mohammadi (2022) may represent the only study specifically addressing their spatial and temporal distribution within the Qom Formation. Given that the characterization and interpretation of non-carbonate petrofacies—including siliciclastic, evaporitic, and volcaniclastic facies—require specialized sedimentological, petrographic, and stratigraphic considerations, the present study is limited to compiling and listing the relevant published studies, as a base work for future studies. Detailed descriptions and independent interpretations of these non-carbonate petrofacies are therefore beyond the scope of the present work. Rare petrofacies of the Qom Formation are summarized in Table 3.

Table 3- Compilation of rare petrofacies reported from the Qom Formation and their depositional settings.

Row	Petrofacies groups	Reports
1	Hybrid facies	Mixed carbonate–siliciclastic petrofacies — Depositional environment not explicitly specified — Bakhshi et al. 2015
2	Red shale	Shallow, restricted lagoon — Mohammadi and Ameri 2018; Mohammadi 2021c
3	Sandstone-bearing petrofacies	Micritic sandstone — Beach — Mohammadi and Ameri 2018; Mohammadi 2021c; Sandstone — Coastal environment — Amirshahkarami and Karavan 2015; Lithic arkose — Not explicitly specified — Bakhshi et al. 2015; Feldspathic lithic arenite — Turbiditic, shallow-to deep-marine — Bakhshi et al. 2015; Litharenite–sublitharenite sandstone petrofacies — Supratidal–intertidal — Karavan et al. 2015; Fine–medium sandstone–calcite-cemented submature litharenite — Barrier/coastal setting — Maghfori Moghadam et al. 2017; sandstone (litharenite) — Turbidity currents — Aftabi Arani et al. 2020;
4	Gravel-bearing petrofacies	Gravel with massive layering and abundant matrix — Fluvial channel / debris flow — Maghfori Moghadam et al. 2017
5	Conglomeratic petrofacies	Conglomeratic petrofacies — Coastal / tidal-flat / upper continental-slope turbiditic settings — Bakhshi et al. 2015; Conglomerate — Continental braided streams — Mohammadi and Ameri 2018; Mohammadi E. 2021a; Mohammadi 2021c; Terrigenous facies (conglomerate and sandstone) — Shallow tidal flat near the coastline — Kiani et al. 2026; Progressive conglomerate — Progressive conglomeratic deposits — Jalali et al. 2017; Conglomeratic petrofacies — channel settings and under turbiditic conditions, — Aftabi Arani et al. 2020;
6	Evaporitic petrofacies	Nodular anhydrite — Supratidal flat / saltern — Khalili et al. 2007; Enterolithic structure — Saltern / playa / dry mudflat–sandflat — Khalili et al. 2007; Anhydrite bedrock — Saltern — Khalili et al. 2007; Anhydrite petrofacies — Restricted lagoon — Jalali et al. 2017; Evaporitic petrofacies — Supratidal — Bakhshi et al. 2015; Evaporite facies (gypsum, anhydrite, and gypsiferous marl) — Saltern / peritidal flat / evaporative beach — Mohammadi and Ameri 2017; Mohammadi 2020b; Evaporites — Saltern — Khalili et al. 2007
7	Volcanic-bearing and volcanic petrofacies	Volcanic arenite — Volcaniclastic setting; the specific environment is not explicitly specified — Bakhshi et al. 2015; Volcanic petrofacies — Volcaniclastic setting; the specific environment is not explicitly specified — Bakhshi et al. 2015

Controls on the formation and distribution of rare microfacies in the Qom Formation

The pronounced lateral facies variability and tectonically controlled depositional setting of the Qom Formation preclude the application of a single depositional model throughout the basin. Instead, previous investigations have demonstrated that carbonate sedimentation took place under a wide range of depositional architectures, reflecting substantial spatial variations in basin morphology, accommodation space, and hydrodynamic conditions.

Accordingly, several depositional models have been proposed for different sectors of the Qom Basin, including carbonate ramps, open shelves, homoclinal ramps, epicontinental shallow-marine platforms, inclined shelves, and rimmed carbonate platforms. Among these, carbonate ramps and open shelves are by far the most frequently recognized depositional systems, indicating that low-gradient carbonate platforms dominated sedimentation during much of the Oligo–Miocene.

In contrast, rimmed carbonate platforms have been documented in only a limited number of studies. To date, this depositional model has been proposed exclusively for five investigated sections, namely the northeastern Garmsar section (Daneshian et al. 2017), the southwestern Semnan section (Karami Movahed et al. 2016), the Arvaneh section in northwestern Semnan (Sabouhi et al. 2012), the Ghalibaf section in northwestern Semnan (Sharifi et al. 2023), and the Mianeh–Bostanabad area of northwestern Iran (Bakhshi et al. 2015). Although these localities represent only a small proportion of the studied sections throughout the Qom Basin, they contain

the majority of the rare microfacies identified in the present synthesis.

According to Mohammadi (2021b), discussion of corals and coral reefs in the Qom Formation commonly evokes the reefal limestones of Member F, which are of Burdigalian age. Although Member F is widely referred to as the "reef member" in the Persian literature, field observations from some sections within the type area, such as the Khurabad section, reveal no clear evidence of laterally continuous reef frameworks; even isolated coral colonies are only rarely observed. Moreover, none of the major studies dealing with the microfacies and palaeoenvironmental evolution of the Qom Formation in the Qom area, i.e. the type area (Okhravi and Amini 1998; Sedighi et al. 2011; Amirshahkarami and Karavan 2015; Mohammadi 2020b), has explicitly invoked a rimmed-shelf model, in which a laterally persistent reefal or barrier framework represents a defining component of the platform margin.

It is noteworthy that Rezaei et al. (2000) also described a microfacies dominated by red algae, with subordinate bryozoan fragments, worm traces, and siliciclastic grains, but lacking corals and foraminifers, as a "reef body". However, they did not invoke a rimmed-shelf model and ultimately interpreted the depositional system as a carbonate ramp. Similarly, Sharifi et al. (2023), from the Ghalibaf section in northwestern Semnan, explicitly interpreted the corals occurring in the coral framestone microfacies as a patch reef, while nevertheless proposing a rimmed carbonate-platform model for the section. The occurrence of ooidal and bioclastic shoals together with patch reefs, however, bears a strong sedimentological resemblance to the carbonate-ramp systems documented from the Asmari Formation (Oligocene–Miocene) of the Zagros Basin, where isolated carbonate buildups and shoal complexes may develop without requiring a laterally continuous reef-rim architecture.

An important observation emerging from this study is that nearly all sections that have been interpreted as rimmed carbonate platforms are of Early Miocene age. These sections collectively contain most of the rare microfacies recognized within the Qom Formation, suggesting a close relationship between platform morphology and the occurrence of uncommon depositional microfacies. The development of a distinct platform margin, together with the establishment of lagoonal, shoal, margin, and slope environments within rimmed platforms, likely generated a greater diversity of ecological niches and sedimentary processes than was possible within relatively homogeneous ramp systems. Consequently, these physiographic and hydrodynamic gradients favored the development and preservation of several microfacies that are absent or extremely uncommon elsewhere in the basin.

The compiled regional dataset further demonstrates that the occurrence of rare microfacies was controlled by both paleogeographic position and depositional environment. Most examples are concentrated along the southern margin of the Central Iranian Desert, particularly in the Semnan–Garmsar region, and in the Mianeh–Bostanabad area of northwestern Iran. These regions evidently represented areas of enhanced environmental heterogeneity during the Early Miocene, promoting the development of specialized carbonate-producing ecosystems and localized depositional settings.

The relatively high occurrence of rare microfacies in these stratigraphic sections is most plausibly related to their marginal position within the Qom carbonate platform and restricted connection with open-marine waters. Their recurrent association with evaporitic facies supports deposition under restricted conditions characterized by limited water exchange and enhanced evaporation. Notably, most sections containing these rare microfacies occur within the known distributional evaporitic domain of the Qom Formation (Mohammadi et al. 2013). Their concentration therefore appears to reflect a broader marginal and restricted-platform facies architecture, rather than being primarily related to preferential sampling or greater research intensity. The apparent rarity of some facies may also reflect diagenetic alteration. Processes such as selective dissolution, cementation, and dolomitization may have obscured or destroyed diagnostic depositional fabrics and skeletal components, resulting in their apparent underrepresentation in the studied sections. Although differences in sampling and petrographic detail may have influenced the recognition of uncommon microfacies, the consistent association of these microfacies with marginal-platform settings, evaporitic facies, and the regional evaporitic domain provides a strong sedimentological basis for linking their occurrence to restricted depositional conditions.

The rare microfacies identified in this study encompass a broad spectrum of depositional environments. Fenestral mudstone, stromatolitic boundstone, and sandy ooid packstone indicate supratidal to intertidal conditions characterized by periodic subaerial exposure and microbial activity. Peloidal packstone represents restricted lagoonal environments, whereas oolitic packstone–grainstone and crinoidal grainstone reflect high-energy shoal complexes. *Neorotalia* packstone and *Operculina* packstone were deposited in outer-shoal to platform-margin settings. In contrast, sandy planktonic foraminiferal wackestone, carbonate breccia, and graded planktonic foraminiferal packstone associated with Bouma sequences record sedimentation along the carbonate slope and in gravity-flow-dominated environments.

These microfacies display limited lateral distribution and relatively narrow vertical ranges, suggesting that their formation was controlled by specific environmental and paleogeographic conditions.

Among all identified rare microfacies, *Neorotalia* packstone represents a distinctive exception. Unlike the majority of the rare microfacies, which are confined to Early Miocene rimmed platforms, this microfacies occurs within Rupelian deposits of the Sanandaj–Sirjan fore-arc basin and is associated with a carbonate ramp depositional system. This globally unique occurrence suggests that its development was primarily controlled by local ecological and paleogeographic conditions rather than by platform morphology alone.

Overall, the results indicate that the distribution of rare microfacies within the Qom Formation reflects the combined influence of depositional environments, carbonate platform architecture, basin evolution, and paleogeographic setting. Consequently, these uncommon microfacies constitute valuable paleoenvironmental indicators and provide important constraints for reconstructing the evolution of Oligo–Miocene carbonate platforms throughout Iran.

Conclusions

This study provides a regional synthesis of the temporal and spatial distribution, depositional environments, and depositional models of rare microfacies within the Oligo–Miocene Qom Formation, based on detailed microfacies analysis of 15 stratigraphic sections and a comprehensive review of previously published studies. The synthesis demonstrates that, in addition to the common and widely distributed facies of the Qom Formation, a diverse assemblage of rare microfacies occurs sporadically and has a strongly restricted spatial and stratigraphic distribution.

The identified rare microfacies record a broad spectrum of depositional environments, ranging from tidal-flat and lagoonal settings to high-energy shoal and platform-margin environments, as well as carbonate-slope and gravity-flow systems. Fenestral mudstone, stromatolitic bindstone, and sandy ooid packstone indicate tidal-flat to locally supratidal–intertidal conditions characterized by episodic subaerial exposure and microbial activity. Peloid-bearing microfacies

https://doi.org/10.22108/jssr.2026.150537.1340

record restricted lagoonal conditions, whereas oolitic grainstone–packstone, ooidal grainstone, and crinoid grainstone reflect relatively high-energy shoal and platform-margin settings. *Neorotalia* packstone and nummulitid packstones represent more open, relatively high-energy settings associated with the outer part of the middle ramp to platform-margin environments. In contrast, graded-bedding and Bouma-sequence packstone, calciturbidite, carbonate breccia, and sandy to silty planktonic foraminiferal microfacies record deposition under gravity-flow and turbiditic conditions along the carbonate slope and adjacent marine settings.

A major outcome of the regional synthesis is the close spatial and temporal association between rare microfacies and rimmed carbonate-platform architecture. Most of the rare microfacies occur in Early Miocene successions, particularly along the Semnan–Garmsar–Qom region and in the Mianeh–Bostanabad area of northwestern Iran. The development of distinct platform margins, together with spatially associated lagoonal, tidal-flat, shoal, reef, and slope environments, produced strong environmental and hydrodynamic gradients that promoted the development and preservation of microfacies that are uncommon or absent in more homogeneous ramp systems. The concentration of these microfacies along the margins of the Qom Formation domain further suggests that the Qom Sea possibly was not continuously connected to the open-marine realm during the Early Miocene. Instead, the regional microfacies pattern is consistent with progressive restriction and eventual closure of the marine connection during this interval.

The regional distribution of rare microfacies also could be controlled by the interaction of paleogeographic position, depositional environment, and carbonate-platform architecture rather than by microfacies processes alone. Restricted lagoonal and peritidal microfacies, high-energy shoal deposits, reefal facies, and slope-related gravity-flow deposits occur in close association within sectors interpreted as rimmed carbonate platforms. This environmental spatial association highlights the importance of platform morphology in generating the accommodation, ecological gradients, and hydrodynamic variability required for the development of diverse and localized carbonate facies.

The *Neorotalia* packstone represents a significant exception to this regional pattern. Unlike most rare microfacies associated with Early Miocene rimmed carbonate platforms, it occurs within Rupelian strata of the Sanandaj–Sirjan forearc basin and is associated with a carbonate-ramp depositional system, specifically a proximal middle-ramp setting. Its occurrence demonstrates that rare microfacies may also develop in response to localized ecological and paleogeographic conditions independent of rimmed-platform architecture.

In addition to rare microfacies, the compiled petrographic record documents restricted occurrences of mixed carbonate–siliciclastic, sandy, gravelly, conglomeratic, evaporitic, and volcanic-bearing petrofacies within the Qom Formation. These petrofacies further emphasize the strong spatial heterogeneity of sedimentation and the sensitivity of the Qom depositional system to changes in accommodation, hydrodynamic conditions, terrigenous input, restriction, and paleogeographic position.

Overall, the results demonstrate that rare microfacies are valuable indicators of localized depositional conditions and carbonate-platform architecture in the Qom Formation. Their regional distribution records the transition from relatively open carbonate-ramp and marine conditions toward increasingly heterogeneous and restricted depositional systems during the Early Miocene. The combined microfacies and petrofacies record therefore provides important constraints on the paleogeographic evolution, environmental differentiation, and progressive restriction of the Oligo–Miocene Qom Basin and offers a regional framework for reconstructing the evolution of carbonate platforms in the Central Iranian domain.

Acknowledgments

We sincerely acknowledge and thank all researchers who have contributed to the study of the the Qom Formation, particularly those whose work was directly drawn upon in the discussion of the rare microfacies. We also extend our heartfelt thanks to everyone who assisted the first author during the fieldwork and study of the 15 measured sections examined in this research.

References

Aftabi Arani A. Ashouri A.R. Daneshian J. Ghaderi A. and Arianasab M.R. 2020. Microfacies analysis, sedimentary environment and sequence stratigraphy of the Qom Formation in the Naraq area. Iranian Joural of Petrolum Geology, 19: 23-44. 20.1001.1.22518738.1399.10.19.4.1

Aftabi Arani A. Ashouri A.R. Daneshian J. Ghaderi A. Wood D.A. 2023. Biostratigraphy, microfacies, and reservoir quality of the Oligocene Qom Formation (Kharzan Section, Northwest of Ardestan, Central Iran). Geological Quarterly 67(3): 1-24. DOI:10.7306/gq.1693

Alsharhan A.S. and Kendall C.G.St.C. 2002. Holocene carbonate/evaporates of Abu Dhabi, and their Jurassic ancient analogs. In: Barth H.J. and Bore B.B. 2002. Sabkha Ecosystems. Kluwer Academic Publisher, Netherlands, 187 - 202.

Amirshahkarami M. and Karavan M. 2015. Microfacies models and sequence stratigraphic architecture of the Oligocene–Miocene Qom Formation, south of Qom City, Iran. Geoscience Frontiers, 6: 593–604. https://doi.org/10.1016/j.gsf.2014.08.004

Anjumshoa A. and Amirshahkarami M. 2014. Biostratigraphy and paleoenvironmental model of the Late Oligocene deposits at the Tanbour section (SW Kerman, Central Iran). Sedimentary Facies, 6: 130–149. 10.22067/sed.facies.v6i2.18099

Arani A. A. A. Ashouri A. R. Daneshian J. Ghaderi A. and Wood D. A. 2023. Biostratigraphy, microfacies, and reservoir quality of the Oligocene Qom Formation (Kharzan Section, Northwest of Ardestan, Central Iran). Geological Quarterly, 67(3): 1–24. 10.7306/gq.1693

Asadi Mehmandosti E. Daneshian J. and Margir N. 2019. Microfacies, depositional environment and diagenetic processes of the Qom Formation in the Khani Abad section, southeast of Kashan. Sedimentary Facies, 12: 1-22. 10.22067/sed.facies.v12i1.70042

Bakhshi A. Liaghat M. and Faizi A. 2015. Microfacies, depositional model, and lithostratigraphy of the Qom Formation in Mianeh–Bostanabad area. Earth Science Research Journal, 21: 19–39. https://doi.org/10.1007/S13146-017-0415-9

Bassi D. Hottinger L. and Nebelsick J.H. 2007. Larger foraminifera from the Upper Oligocene of the Venetian area, north-east Italy. Palaeontology, 50(4): 845-868. https://doi.org/10.1111/j.1475-4983.2007.00677.x

Beavington-Penney S.J. and Racey A. 2004. Ecology of extant nummulitids and other larger benthic foraminifera: Applications in palaeoenvironmental analysis. Earth-Science Reviews, 67(3-4): 219-265. 10.1016/j.earscirev.2004.02.005

Behforouzi E. Safari A. and Vaziri-Moghaddam H. 2010. Microfacies analysis and depositional environment interpretation of the Qom Formation in the Chenar area (northwestern Kashan). Sedimentary Facies, 2: 143–152.

BouDagher-Fadel M.K. 2018. Evolution and geological significance of larger benthic foraminifera, second edition. UCL Press, London, 702 p.

Bouma A. H. 1962. Sedimentology of some flysch deposits. Elsevier, Amsterdam, 168 p.

Brandano M. and Corda L. 2002. Nutrients, sea level and tectonics: Constrains for the facies architecture of a Miocene carbonate ramp in central Italy. Terra Nova, 14: 257-262. https://doi.org/10.1046/j.1365-3121.2000.00419.x

Brandano M. Frezza V. Tomassetti L. Pedley M. and Matteucci R. 2009. Facies analysis and palaeoenvironmental interpretation of the Late Oligocene Attard Member (Lower Coralline Limestone Formation), Malta. Sedimentology, 56: 1138-1158. https://doi.org/10.1111/j.1365-3091.2008.01023.x

Brandano M. Mateu-Vicens G. and Baceta J.I. 2022. Understanding carbonate factories through palaeoecological and sedimentological signals – Tribute to Luis Pomar. Sedimentology, 69(1): 5-23. https://doi.org/10.2110/sepmscn.058.02

Daneshian J. Asadi Mehmandosti E. and Ramezani Dana L. 2017. Microfacies, sedimentary environment and sequence stratigraphy of the Qom Formation, Deh Namak, northwest of Garmsar, Iran. Iranian Journal of Geology, 41: 23–43.

Daneshian J. Mosadegh H., Khalaj H. and Ghasemi A. 2008. Sequence stratigraphy of the Qom Formation in the type locality (Kuh-e Bichareh), SE Qom, north of Central Iran. Journal of Basic Sciences, 34: 19–54.

Daneshian J. Shahrabi M. and Akhlaghi M. 2010. Biostratigraphy and paleoenvironment of the Qom Formation deposits in NE Mahneshan. Geoscience, 76: 45-50. 10.22071/gsj.2010.55643

Dehghan R. Safari A. and Vaziri-Moghaddam H. 2010. Analysis of microfacies and depositional environments of the Qom Formation in Ghohroud area (southern Kashan). Research in Earth Sciences, 3: 60–73. https://doi.org/10.1007/S13146-017-0415-9

Dunham R. J. 1962. Classification of carbonate rocks according to depositional texture. In: Ham W. E. (Ed.), Classification of Carbonate Rocks. American Association of Petroleum Geologists Memoir 1: 108–121.

Embry A. F. and Klovan J. E. 1971. A Late Devonian reef tract on northeastern Banks Island, Northwest Territories. Bulletin of Canadian Petroleum Geology, 19: 730–781.

FaizNia S. and Mosafi H.R. 1998. Microfacies and depositional environment of the Qom Formation in Semnan region. Geoscience, 27–28: 64-77. [In Persian]

Flügel E. 2010. Microfacies analysis of limestone. Springer, Berlin, 984pp.

Ghaedi M. Mohammadi E. Peixoto B. Bahrami A. Salahi M. A. and Yazdi M. 2026. Gastrochaenolites borings from Iran: Paleoenvironmental and bioerosional implications. Ichnos. DOI: 10.1080/10420940.2026.2726230.

Geel T. 2000. Recognition of stratigraphic sequences in carbonate platform and slope deposits: Empirical models based on microfacies analysis of Palaeogene deposits in southeastern Spain. Palaeogeography, Palaeoclimatology, Palaeoecology, 155: 211–238. 10.1016/S0031-0182(99)00117-0

Hallock P. 1984. Distribution of selected species of living algal symbiont-bearing foraminifera on two Pacific coral reefs. Journal of Foraminiferal Research, 14: 250–261.

Hallock P. Glenn E.C. and Muller P.H. 1986. Larger Foraminifera: A tool for paleoenvironmental analysis of Cenozoic carbonate depositional facies. Palaios, 1: 55–64.

Hassanzadeh S. Adabi M.H. Kohansal Ghadimvand N. Jalali M. and Arian M.A. 2020. Facies analysis and stratigraphic sequence architecture in a back-arc basin in central Iran: A case study from the Early Miocene of the Qom Formation. Periódico Tchê Química, 17(35): 135-154.

Holakouee Z. Maghfouri Moghaddam I. Yazdi M. and Yousefi Yeganeh B. 2018. Biostratigraphy and microfacies of Qom Formation in Urumieh-Dokhtar Zone, Iran. International Journal of Engineering and Technology, 10(4): 1052-1066. DOI:10.21817/ijet/2018/v10i4/181004216

Hoseini Nejad S.M. Rameh H. and Aharipour R. 2016. Biostratigraphy and depositional environment of the Qom Formation in Talan Kuh section, SW Semnan. Applied Sedimentology, 7: 101-116.

Hottinger L. 1983. Processes determining the distribution of larger Foraminifera in space and time. Utrecht Micropaleontological Bulletin, 30: 239–253.

Hottinger L. 1997. Shallow benthic foraminiferal assemblages as signals for depth of their deposition and their limitations. Bulletin de la Société géologique de France, 168: 491–505.

Jalali M. Sadeghi A. and Adabi M. H. 2016. Microfacies, depositional environment and sequence stratigraphy of the Qom Formation in East Siyah Kuh surface section (south of Garmsar). Iranian Journal of Geology, 39: 83–102.

Jalali M. Sadeghi A. and Adabi M. H. 2017. Microfacies, sedimentary environment and sequence stratigraphy of the Qom Formation in Yort-e Shah No. 1 well and Morreh Kuh surface section (South of Tehran). Journal of Stratigraphy and Sedimentology Research, 33: 25–48. 10.22108/JSSR.2017.21138

Karami-Movahed F. Aleali M. and Ghazanfari P. 2016. Facies analysis, depositional environment and diagenetic features of the Qom Formation in the Saran Semnan, Central Iran. Open Journal of Geology, 6: 349–362. 10.4236/ojg.2016.66030

Karavan M. Mahboubi A. Vaziri-Moghaddam H. and Moussavi-Harami R. 2015. Sedimentary facies and sequence stratigraphy of the Qom Formation deposited in northeast of Delijan, northwest of Central Iran. Geosciences Journal, 94: 237–248. 10.22071/gsj.2015.42663

Khaksar K. 2020. Biostratigraphy and paleoecology research on Qom Formation based on microfossils at East of the Qom. Geosciences, 115: 187–198. 10.22071/gsj.2020.108181

Khalili M. Beavers R. and Torabi H. 2007. Depositional environment of the evaporitic unit (D-member) of the Qom Formation (Central Iran). Carbonates and Evaporites, 22: 101–112.

Kiani A. Saberi M. H. and Rabbani A. R. 2026. Evaluation of the hydrocarbon system of Qom Formation in the North of Dasht-e-Kavir, Central Iran. Journal of Petroleum Exploration and Production Technology, 16: 38. https://doi.org/10.1007/s13202-026-02138-4

Lázár B. Á. Falahatgar M. Sarfi M. and Kallanxhi M. E. 2023. Biostratigraphy and paleoenvironmental analysis of the Lower Miocene Qom Formation (Jaam area, Central Iranian Basin). Rivista Italiana di Paleontologia e Stratigrafia, 129: 609–628.

Maghfori Moghadam I. Holakouee Z. Yazdi M. and Yousefi B. 2017. Biofacies analysis of the Upper Oligocene deposits (Qom Formation) in Urumieh–Dokhtar Zone, Iran. Anuário do Instituto de Geociências, 40: 163–179. https://doi.org/10.11137/2017_2_163_179

Mahyad M. Safari A. Vaziri-Moghaddam H. and Seyrafian A. 2018. Reconstruction of sedimentary environment, and depositional sequences based on microfacies of the Qom Formation in the Kahak area (southwest of Qom city). Iranian Journal of Petroleum Geology, 15: 32-48. 20.1001.1.22518738.1397.8.15.3.8

Mahyad M. Safari A. Vaziri-Moghaddam H. and Seyrafian A. 2019. Biofacies, taphofacies and depositional environments in the north of Neotethys Seaway (Qom Formation, Miocene, Central Iran). Russian Geology and Geophysics, 60: 1368–1384. https://doi.org/10.15372/RGG2019133

Mohammadi E. 2020a. Foraminiferal morphogroups of the Qom Formation in E Sirjan and SW Kashan: implication for paleoenvironmental and paleoecological interpretations. Iranian Journal of Petroleum Geology, 20: 82–94 [In

Persian].
Mohammadi E. 2020b. Sedimentary facies and depositional environments of the Oligocene–Early Miocene marine Qom Formation, Central Iran Back-Arc Basin, Iran (northeastern margin of the Tethyan Seaway). Carbonates and Evaporites, 35: 1–29. https://doi.org/10.1007/s13146-020-00553-0
Mohammadi E. 2020c. Sequence stratigraphy of the Qom Formation in the Sirjan–Abadeh region. Journal of Stratigraphy and Sedimentology Researches, 37(1): 67–94 [In Persian]. 10.22108/JSSR.2020.120992.1142
Mohammadi E. 2021a. Conglomerate and sandstones of the Qom Formation: temporal and spatial distribution and depositional environments. In: Proceedings of the 14th Symposium of the Iranian Paleontological Society, Graduate University of Advanced Technology, Kerman, 79–90.
Mohammadi E. 2021b. Oligo–Miocene coral reefs. In: Proceedings of the 14th Symposium of the Iranian Paleontological Society, Graduate University of Advanced Technology, Kerman, 91–97.
Mohammadi E. 2021c. Sedimentary facies and paleoenvironmental interpretation of the Oligocene larger-benthic-foraminifera-dominated Qom Formation in the northeastern margin of the Tethyan Seaway. Palaeoworld, 30: 356–372. 10.1016/j.palwor.2020.06.005
Mohammadi E. 2021d. Sequence stratigraphy of the Qom Formation in the Natanz–Qom region. Advanced Applied Geology, 18: 113–132 [In Persian]. 10.22084/psj.2021.23642.1272
Mohammadi E. 2022. Temporal and spatial distribution of the Qom Formation pyroclastic deposits with special emphasis on SE Kerman Province: their application in (tephra) event stratigraphy. Journal of Stratigraphy and Sedimentology Researches, 87: 117–134.
Mohammadi E. 2023a. Foraminiferal biozonation, biostratigraphy, and trans-basinal correlation of the Oligo–Miocene Qom Formation, Iran (northeastern margin of the Tethyan Seaway). Palaeoworld. DOI: 10.1016/j.palwor.2022.04.005.
Mohammadi E. 2023b. Introducing the newly-established "Varkan Member" in SW Kashan as the oldest member of the Qom Formation. Advanced Applied Geology, 13(1): 364–383. 10.22055/aag.2022.41562.2308
Mohammadi E. 2024a. Hydrocarbon potential and petroleum system of the Oligo–Miocene Qom Formation, Iran: a review. In: Proceedings of the 4th International World Energy Conference (IWEC), Kayseri, Türkiye, 778–785.
Mohammadi E. 2024b. Re-examination of biostratigraphy and age interpretations in the Sanandaj–Sirjan and Central Iran basins (NE margin of the Tethyan Seaway). Journal of Foraminiferal Research, 54: 202–216. https://doi.org/10.61551/gsjfr.54.3.202
Mohammadi E. 2027. Facies architecture and paleoenvironmental signatures of the Oligocene Qom Formation in an active marginal marine setting. Boletín de la Sociedad Geológica Mexicana, 79(1).
Mohammadi E. and Ameri H. 2015. Biotic components and biostratigraphy of the Qom Formation in northern Abadeh, Sanandaj–Sirjan fore-arc basin, Iran (northeastern margin of the Tethyan Seaway). Arabian Journal of Geosciences, 8: 10789–10802. https://doi.org/10.1007/s12517-015-1948-7
Mohammadi E. and Ameri H. 2017. Microfacies analysis and depositional model of the Qom Formation in the Khurabad area (southeastern Qom). Researches in Earth Sciences, 28: 37–58 [In Persian].
Mohammadi E. and Ameri H. 2018. Facies, depositional environment and depositional model of the Qom Formation in northern Abadeh (Sanandaj–Sirjan fore-arc basin). Sedimentary Facies, 26: 30 p. [In Persian].
Mohammadi E. and Ameri H. 2024. Foraminiferal biostratigraphy and paleoecology of the southeasternmost outcrops of the Oligocene Qom Formation, SE Iran. Journal of the Geological Society of India,100(1):115-126. https://doi.org/10.17491/jgsi/2024/172988
Mohammadi E. Ameri H. Ghaedi M. Vaziri M. R. Dastanpour M. and Sadeghi R. 2016. Biostratigraphy, microfacies and depositional model of the Qom Formation in northeastern Natanz (southeastern Qom back-arc basin). Paleontology, 3: 1–24 [In Persian].
Mohammadi E. and Ghaedi M. 2024. Diversity and paleoecological significance of zooxanthellate corals of Oligocene Qom Formation, SE Iran. Earth Sciences Research Journal, 28: 127–137.
Mohammadi E. Ghaedi M. Rameh H. Sadeghi R. Ahmadi T. and Vaziri M. R. 2022. Foraminiferal morphogroups of the Qom Formation in the Natanz and Qom regions: implication for paleoenvironmental and paleoecological interpretations. Advanced Applied Geology, 12(1): 75–89 [In Persian]. https://aag.scu.ac.ir/article_16799_e511794a56ee3dc88e63040ab1d8cc89.pdf
Mohammadi E. Hasanzadeh-Dastgerdi M. Ghaedi M. Dehghan R. Safari A. Vaziri-Moghaddam H. Baizidi C. Vaziri M. and Sfidari E. 2013. The Tethyan Seaway Iranian Plate Oligo–Miocene deposits (the Qom Formation): distribution of Rupelian (Early Oligocene) and evaporate deposits as evidences for timing and trending of opening and closure of the Tethyan Seaway. Carbonates and Evaporites, 28: 321–345. https://doi.org/10.1007/s13146-012-0120-7
Mohammadi E. Hasanzadeh-Dastgerdi M. Safari A. and Vaziri-Moghaddam H. 2019. Microfacies and depositional environments of the Qom Formation in Barzok area, SW Kashan, Iran. Carbonates and Evaporites, 34: 1293–1306. https://doi.org/10.1007/s13146-017-0415-9
Mohammadi E. and Sadeghi R. 2024. The lower parts of the Oligo–Miocene Qom Formation in the Kegharaki (SE Jiroft) and Shurab (SE Qom) areas: biostratigraphy, microfacies, and depositional environments. Journal of Stratigraphy and Sedimentology Researches, 97: 23–40. 10.22108/JSSR.2024.140914.1280
Mohammadi E. Safari A. Vaziri-Moghaddam H. and Mohammadi Monfared M. 2009. Microfacies analysis and depositional environment of the Qom Formation in the Jazeh area (South of Kashan). Sedimentary Facies, 2: 81-94. 10.22067/sed.facies.v2i1.823
Mohammadi E. Safari A. Vaziri-Moghaddam H. Vaziri M. R. and Ghaedi M. 2011. Microfacies analysis and paleoenvironmental interpretation of the Qom Formation, south of Kashan, central Iran. Carbonates and Evaporites, 26: 255–271. 10.1007/s13146-011-0059-0
Mohammadi E. Vaziri M. R. and Dastanpour M. 2014. Microfacies analysis and depositional environment reconstruction of the Qom Formation, Sirjan area, southwest of Kerman. Journal of Stratigraphy and Sedimentology Researches, 55: 35–54 [In Persian]. 20.1001.1.20087888.1393.30.2.3.2
Mohammadi E. Vaziri M. R. and Dastanpour M. 2015. Biostratigraphy of the Nummulitids and Lepidocyclinids-bearing Qom Formation based on larger benthic foraminifera (Sanandaj–Sirjan fore-arc basin and Central Iran back-arc basin, Iran). Arabian Journal of Geosciences, 8: 403–423. https://doi.org/10.1007/s12517-013-1136-6
Mohammadi M. Kohansal Ghadimvand N. Vaziri S.H. and Moosavian M. 2009. Microfacies and sedimentary environments of the Qom Formation in Vieh section, S Saveh. Journal of Sediment and Sedimentary Rock, 4: 35-44.
Mohammadian M. Safari A. and Vaziri-Moghaddam H. 2013. Microfacies analysis and depositional environment of Qom Formation in the Bijegan area (northeast of Delijan). Sedimentary Facies, 6: 65-76. 10.22067/sed.facies.v6i1.13021
Navavajary Sh. Maghfouri Moghadam I. Shahidi A. R. and

Nazari H. 2021. Microbiostratigraphy and paleoenvironment of Oligo–Miocene deposits in the North of Central Iran. Geosciences, 119: 37–50. 10.22071/gsj.2020.243135.1833

Noroozpour H. 2021. A report from the Oligocene Qom Formation benthic foraminifera; northwest of the Sanandaj–Sirjan Zone, western Iran. Carbonates and Evaporites, 39: 1–11. https://doi.org/10.1007/s13146-021-00710-z

Noori M. Zohdi A. Kouhestani H. Nabatian Gh. and Mokhtari M.A.A. 2018. Lithostratigraphy, microfacies and sedimentary environment of the Qom Formation at Madabad celestite deposit, south of Zanjan. Sedimentary Facies, 11: 288-303.

Nouradini M. Azami S. H. Hamad M. Yazdi M. and Ashouri A. R. 2015. Foraminiferal paleoecology and paleoenvironmental reconstructions of the lower Miocene deposits of the Qom Formation in Northeastern Isfahan, Central Iran. Boletín de la Sociedad Geológica Mexicana, 67: 59–73.

Okhravi R. and Amini A. 1998. An example of mixed carbonate-pyroclastic sedimentation (Miocene, Central Basin, Iran). Sedimentary Geology, 118: 37–57.

Piller W. E. Harzhauser M. Kranner M. Mandic O. Mohtat T. and Daneshian J. 2024. The Tethyan Seaway during the early to middle Miocene: new data and a review. Gondwana Research, 135: 57–74. https://doi.org/10.1016/j.gr.2024.08.004

Pomar L. 2001. Ecological control of sedimentary accommodation: Evolution from a carbonate ramp to rimmed shelf, Upper Miocene, Balearic Islands. Palaeogeography, Palaeoclimatology, Palaeoecology, 175: 249–272. DOI: 10.1016/S0031-0182(01)00375-3.

Rabbani J. Mirzaie Ataabadi M. and Shaahsavari E. 2020. Microfacies, sedimentary environmental model and relative sea level change of marly strata of the Qom Formation in Zarrin-Abad section, South of Zanjan. Journal of Stratigraphy and Sedimentology Researches, 36(1): 115-134. https://doi.org/10.22108/jssr.2020.120140.1128

Rahiminejad A. H. Yazdi M. and Ghosh A. K. 2022. Paleoecology of Lower Miocene coralline red algae-rich grainstone facies in the Qom Formation (Vartun section, Central Iran). Boletín de la Sociedad Geológica Mexicana, 74: 1–16. https://doi.org/10.18268/bsgm2022v74n2a020122

Rahimzadeh F. 1994. Geology of Iran: Oligocene–Miocene, Pliocene. Geological Survey of Iran, 311pp. [In Persian]

Rasser M.W. Scheibner C. and Mutti M. 2005. A paleoenvironmental standard section for Early Ilerdian tropical carbonate factories (Corbieres, France; Pyrenees, Spain). Facies 51, 218–232. https://doi.org/10.1007/s10347-005-0070-9

Rezaei M. R. Honarmand J. and Okhravi R. 2000. Microfacies and depositional environments of the Qom Formation in Alborz anticline, Qom Basin, Central Iran. Basic Sciences Journal of Tehran University, 2: 139–156.

Romero J. Caus E. and Rosell J. 2002. A model for the palaeoenvironmental distribution of larger foraminifera based on late Middle Eocene deposits on the margin of the South Pyrenean basin (NE Spain). Palaeogeography, Palaeoclimatology, Palaeoecology, 179: 43–56. 10.1016/S0031-0182(01)00406-0

Sabouhi M. Sheykh M. Naghavi Azad M. and Mohammadi M. 2012. Facies and depositional environment of Qom Formation in Arvaneh area (Semnan). Quarterly Journal of Sediment and Sedimentary Rocks, 1–14.

Safari A. Ghanbarloo H. Esfahani M. M. and Vaziri-Moghaddam H. 2020a. Age determination of the Oligocene Qom Formation and interpretation of palaeoenvironments in the Qom back-arc basin (northern Neotethys) using benthic foraminifera. Zeitschrift der Deutschen Gesellschaft für Geowissenschaften, 171: 503–519.

Safari A. Ghanbarloo H. Kasiri A. and Mahmudi Purnajjari S. 2020b. Sedimentary environment and depositional sequences of the Oligocene Qom Formation in Central Iran based on microfacies and microtaphofacies analysis. Carbonates and Evaporites, 35: 100, 1–22. DOI: 10.1007/s13146-020-00633-1.

Safari A. Ghanbarloo H. and Mohammadi E. 2020c. Microfacies, sedimentary environment, and sequence stratigraphy of the Qom Formation in the Maragh area (Southwest of Kashan). Iranian Journal of Petroleum Geology, 20: 41–61.

Safari A. Mohammadi E. and Ameri H. 2014. Analysis of the Qom Formation microfacies and controlling factors on their deposition, Varkan area (Southwest of Kashan), Sanandaj–Sirjan fore-arc basin. Paleontology, 2: 187–204 [In Persian].

Sarkar S. Allameh M. Nasiri Y. and Hadi M. 2025. Palaeogeographical implications of an ecological paradox: cool-water carbonates in an Early Miocene mid-latitude warm realm (Qom Formation, Central Iran). Lethaia, 58:1-19. https://doi.org/10.18261/let.58.1.6

Sarkar S. Ghosh A.K. and Rao G.M.N. 2016. Coralline algae and benthic foraminifera from the Long Formation (Middle Miocene) of the Little Andaman Island, India: Biofacies analysis, systematics and palaeoenvironmental implications. Journal of the Geological Society of India, 87: 69–84. https://doi.org/10.1007/s12594-016-0375-z

Seddighi M. Vaziri-Moghaddam H. Taheri A. and Ghabeishavi A. 2011. Depositional environment and constraining factors on the facies architecture of the Qom Formation, Central Basin, Iran. Historical Biology: 1–10. DOI: 10.1080/08912963.2011.580434.

Seyrafian A. Torabi H. and Shojaei M. 2006. Microfacies and depositional environment of the Qom Formation in Nazanz Area (Charkha Mountain). Basic Sciences Research Journal of Isfahan University, 23: 135–148.

Seyrafian A. and Torabi H. 2005. Petrofacies and sequence stratigraphy of the Qom Formation (Late Oligocene–Early Miocene?), north of Nain, southern trend of the Central Iranian Basin. Carbonates and Evaporites, 20: 82–90. https://doi.org/10.1007/BF03175451

Sharifi J. Nasiri Y. Badpa M. Taghdisi Nikbakht S. Sarkar S. and Hadi M. 2023. Depositional environment and sequence stratigraphy of the Qom Formation (Miocene) from the Ghalibaf section, Central Iran. Boletín de la Sociedad Geológica Mexicana, 75: A061023. DOI: 10.18268/BSGM2023v75n3a061023.

Sharifi-Yazdi M. Ćorić S. Wolfgring E. and Wagreich M. 2025. Calcareous nannofossils, stable isotopes, and cyclostratigraphy of the upper Qom Formation (Burdigalian, Central Iran): implications for paleoclimate and paleoecology. Palaeogeography, Palaeoclimatology, Palaeoecology, 676: 113171. 10.1016/j.palaeo.2025.113171

Vaziri-Moghaddam H. and Torabi H. 2004. Biofacies and sequence stratigraphy of the Oligocene succession, Central Basin, Iran. Neues Jahrbuch für Geologie und Paläontologie, Abhandlungen, 6: 321–334. 10.1127/njgpm/2004/2004/321

Wilson J. L. 1975. Carbonate Facies in Geologic History. Springer-Verlag, Berlin, Heidelberg, New York, 471 p.

Wilson J. L. 2013. Carbonate Facies in Geologic History. Springer, Berlin, 471 p.

Yazdi Moghadam M. Sarfi M. Sharifi M. and Taghipour A. 2023. Postmiogypsinella intermedia Sirel and Gedik 2011 from the upper Oligocene of Central Iran (Qom Formation): paleogeography and paleoenvironmental implications. Journal of Palaeogeography, 12(2):246-262. 10.1016/j.jop.2023.02.002